

Convergence of stochastic structure-preserving schemes for computing effective diffusivity in random flows

Junlong Lyu^a, Zhongjian Wang^a, Jack Xin^b, Zhiwen Zhang^{a,*}

^a*Department of Mathematics, The University of Hong Kong, Pokfulam Road, Hong Kong SAR, China.*

^b*Department of Mathematics, University of California at Irvine, Irvine, CA 92697, USA.*

Abstract

In this paper, we propose stochastic structure-preserving schemes to compute the effective diffusivity for particles moving in random flows. We first introduce the motion of particles using the Lagrangian formulation, which is modeled by stochastic differential equations (SDEs). We also discuss the definition of the corrector problem and effective diffusivity. Then we propose stochastic structure-preserving schemes to solve the SDEs and provide a sharp convergence analysis for the numerical schemes in computing effective diffusivity. The convergence analysis follows a probabilistic approach, which interprets the solution process generated by our numerical schemes as a Markov process. By using the central limit theorem for the solution process, we obtain the convergence analysis of our method in computing long time solutions. Most importantly our convergence analysis reveals the connection of discrete-type and continuous-type corrector problems, which is fundamental and interesting. We present numerical results to demonstrate the accuracy and efficiency of the proposed method and investigate the convection-enhanced diffusion phenomenon in two- and three-dimensional incompressible random flows.

AMS subject classification: 35B27, 47J07, 60F05, 60H35, 65P10, 65M75.

Keywords: Convection-enhanced diffusion; effective diffusivity; stochastic Hamiltonian systems; random flows; corrector problem; central limit theorem; Markov process.

1. Introduction

In this paper, we study the diffusion enhancement phenomenon for particle motions in random flows, which is described by the following passive tracer model, i.e., a stochastic differential equation (SDE) with a random drift,

$$d\mathbf{X}(t) = \mathbf{b}(t, \mathbf{X}(t), \omega)dt + \sigma d\mathbf{w}(t), \quad \mathbf{X}(0) = 0, \quad (1)$$

where $\mathbf{X}(t) \in R^d$ is the position of the particle, $\sigma > 0$ is the molecular diffusivity, and $\{\mathbf{w}(t)\}_{t \geq 0}$ is the standard d -dimensional Brownian motion. Here the velocity field $\mathbf{b}(t, \mathbf{X}(t), \omega)$

*Corresponding author

Email addresses: u3005480@connect.hku.hk (Junlong Lyu), ariswang@connect.hku.hk (Zhongjian Wang), jxin@math.uci.edu (Jack Xin), zhangzw@hku.hk (Zhiwen Zhang)

is modeled by a random field in order to mimic the energy spectra of the turbulent flow [11, 13]. Specifically, we assume $\mathbf{b}(t, \mathbf{X}(t), \omega)$ is a zero mean, jointly stationary, ergodic random vector field over a certain probability space, where ω is an element of the probability space describing all possible environments. The randomness in $\mathbf{b}(t, \mathbf{X}(t), \omega)$ is independent of the randomness in the Brownian motion $\mathbf{w}(t)$. In addition, we assume that the realizations of $\mathbf{b}(t, \mathbf{X}(t), \omega)$ are almost surely divergence free, i.e. $\nabla \cdot \mathbf{b}(t, \mathbf{X}(t), \omega) = 0$. Furthermore, in order to guarantee the existence of the solution to (1), we assume that $\mathbf{b}(t, \mathbf{X}(t), \omega)$ is almost surely locally Lipschitz in \mathbf{X} . We emphasize that since any statement, such as the effective diffusivity, involving statistical properties of the solution $\mathbf{X}(t)$ requires only convergence in law, the regularity assumption on the velocity field is natural and will facilitate our algorithm design and convergence analysis in this paper.

We are interested in studying the long-time large-scale behavior of the particles $\mathbf{X}(t)$ in (1). Namely, whether the motion of the particles $\mathbf{X}(t)$ has a long time diffusive limit? More specifically, let $X_\epsilon(t) \equiv \epsilon X(t/\epsilon^2)$ denote the rescaled process of (1). We want to find conditions under which $X^\epsilon(t)$ converges in law, as $\epsilon \rightarrow 0$, to a Brownian motion $\mathbf{w}_1(t)$ with a certain covariance matrix $D^E \in R^{d \times d}$, where D^E is called the effective diffusivity matrix. This problem is referred to as the homogenization of time-dependent flow problem.

Computing the effective diffusivity matrix D^E (i.e., homogenization of time-dependent flows) has been widely studied under various conditions on the flows. For spatial-temporal periodic velocity fields and random velocity fields with short-range correlations, one can apply the homogenization theory [1, 7, 8, 14] to compute the effective diffusivity matrix D^E , where D^E can be expressed in terms of particle ensemble average (Lagrangian framework) or an average of solutions to corrector problems (Eulerian framework).

The dependence of D^E on the velocity field of the problem is highly nontrivial. For time-independent Taylor-Green flows, the authors of [15] proposed a stochastic splitting method and calculated the effective diffusivity in the limit of vanishing molecular diffusion. For time-dependent chaotic flows, we proposed a Lagrangian-type numerical integrator to compute the effective diffusivity using structure-preserving schemes [19]. In the subsequent work [18], we provided a sharp and uniform-in-time error estimate for the numerical integrator in computing the effective diffusivity. However, we point out that the method and the convergence analysis obtained in [19, 18] were designated for flows generated from separable and deterministic Hamiltonian only.

For random flows with long-range correlations, the long-time large-scale behavior of the particle motion is complicated and difficult to study in general, since various forms of anomalous diffusion, such as super-diffusion and sub-diffusion may exist. The interested reader is referred to the review paper [13], where some anomalous diffusion was obtained for exactly solvable models, i.e. shear flows generated from separable Hamiltonian

There are several theoretical works on homogenization of time-dependent random flows. Such results include, among others, in [2], the authors proved the existence of the effective diffusivity for a two-dimensional time-dependent incompressible Gaussian velocity field. In [12, 10], the authors proved the homogenization of convection-diffusion in a time-dependent,

ergodic, incompressible random flow. In [6, 5], the authors proved some necessary conditions under which the long-time behavior for convection-diffusion in a turbulent flow is diffusive. Those results show that the dependence of the effective diffusivity upon the molecular diffusion σ and the velocity field \mathbf{b} in the random flow is complicated and how to describe this dependence is very difficult in general. Additionally, it seems difficult to study the existence of residual diffusivity for the passive tracer model (1). The residual diffusivity refers to the non-zero effective diffusivity in the limit of zero molecular diffusion σ .

This motivates us to develop robust numerical schemes so that we can compute the effective diffusivity of random flows. Notice that these random flows are generated from non-separable Hamiltonians, which are much more difficult than the problems studied in [13, 19]. In this work, we first propose an implicit structure-preserving scheme to solve the SDE (1), in order to deal with the non-separable Hamiltonian. Second, we provide a sharp error estimate for the numerical scheme in computing effective diffusivity. Our analysis is based on a probabilistic approach. We interpret the solution process generated by our numerical scheme as a Markov process, where the transition kernel can be constructed according to the numerical scheme in solving (1). By exploring the ergodicity of the solution process and using the central limit theorem for Markov process, we obtain a sharp convergence analysis for our method. Most importantly, our convergence analysis reveals the connection of discrete-type and continuous-type corrector problems, which is fundamental and interesting. Finally, we present numerical results to demonstrate the accuracy of the proposed method in computing effective diffusivity for several incompressible random flows in both two- and three-dimensional space.

To the best of our knowledge, this paper appears to be the first one in the literature to develop Lagrangian numerical methods to compute effective diffusivity in random flows through the connection with Eulerian corrector problem. The probabilistic approach in the convergence analysis takes into account the ergodic nature of the solution process and leads to a sharp error estimate. Notice that if one chooses the Gronwall inequality in the error estimate, one cannot get rid of the exponentially growth pre-factor in the error term, which makes the estimate not sharp. Moreover, stochastic structure-preserving Lagrangian scheme enables us to investigate the convection-enhanced diffusion phenomenon in random flows. Especially, we can numerically study the dependence of the effective diffusivity in the regime of molecular diffusion σ and the setting of the velocity field \mathbf{b} in the random flow.

The rest of the paper is organized as follows. In Section 2, we briefly review some existing results for diffusion in random flows and introduce the definition of effective diffusivity by solving a continuous-type corrector problem. In Section 3, we propose our stochastic structure-preserving schemes in computing effective diffusivity for the passive tracer model (1). In Section 4, we provide the convergence analysis for the proposed method based on a probabilistic approach. In addition, we prove the equivalence of the definition of the effective diffusivity through the discrete-type and continuous-type corrector problems. In Section 5, we present numerical results to demonstrate the accuracy and efficiency of our method. Concluding remarks are made in Section 6.

2. Preliminaries

To make this paper self-contained, we give a brief review of existing results on convection-enhanced diffusion in random flows and the effective diffusivity. Since these are standard results, we adopt the notations that were used in [6, 5].

2.1. Some formulations and results for diffusion in random flows

Let $(\mathcal{X}, \mathcal{H}, P_0)$ be a probability space. Let $\tau_{\mathbf{x}}, \mathbf{x} \in \mathbf{R}^d$ be an almost surely continuous, jointly measurable group of measure preserving transformation of \mathcal{X} with the following properties:

- (T1) $\tau_{\mathbf{0}} = Id_{\mathcal{X}}$ and $\tau_{\mathbf{x}+\mathbf{y}} = \tau_{\mathbf{x}}\tau_{\mathbf{y}}, \forall \mathbf{x}, \mathbf{y} \in \mathbf{R}^d$.
- (T2) The mapping $(\chi, \mathbf{x}) \mapsto \tau_{\mathbf{x}}\chi$ is jointly measurable.
- (T3) $P_0(\tau_{\mathbf{x}}(A)) = P_0(A)$, for $\mathbf{x} \in \mathbf{R}^d, A \in \mathcal{H}$.
- (T4) $\lim_{\mathbf{x} \rightarrow \mathbf{0}} P_0(\chi : |f \circ \tau_{\mathbf{x}}(\chi) - f(\chi)| \geq \eta) = 0, \forall f \in L^2(\mathcal{X})$ and $\forall \eta > 0$.
- (T5) If $P_0(A\Delta\tau_{\mathbf{x}}(A)) = 0, \forall \mathbf{x} \in \mathbf{R}^d$, then A is a trivial event, i.e., $P_0(A)$ is either 0 or 1.

One can verify that $\tau_{\mathbf{x}}$ induces a strongly continuous group of unitary mapping $U^{\mathbf{x}}$ on $L^2(\mathcal{X})$, which satisfies

$$U^{\mathbf{x}}f(\chi) = f(\tau_{\mathbf{x}}(\chi)), \quad f \in L^2(\mathcal{X}), \quad \mathbf{x} \in \mathbf{R}^d. \quad (2)$$

In addition, it is easily to find that the group $U^{\mathbf{x}}$ has d independent, skew-adjoint generators $D_k : \mathcal{D}_k \rightarrow L^2(\mathcal{X})$ corresponding to directions $\mathbf{e}_k, k = 1, \dots, d$.

We introduce some function spaces that are useful in the analysis. Let $C_b^m(\mathcal{X})$ be the space of functions f in the intersection of the domains of D_k^n with $\|D_k^n f\|_{L^\infty(\mathcal{X})} < +\infty, k = 1, \dots, d, n = 1, \dots, m$. It is well known that $C_b^\infty(\mathcal{X}) = \cap_{m \geq 1} C_b^m(\mathcal{X})$ is dense in $L^p(\mathcal{X}), 1 \leq p < +\infty$; see [3]. Let $L_0^2(\mathcal{X}) = \{f \in L^2(\mathcal{X}) | \mathbf{E}_0 f = 0\}$, where \mathbf{E}_0 is the expectation associated with the probability measure P_0 .

Let Ω be the space of \mathcal{X} -valued continuous function $C([0, \infty); \mathcal{X})$ and let ℓ be its Borel σ -algebra. Let $P^t, t \geq 0$, be a strongly continuous Markov semigroup on $L^2(\mathcal{X})$, which satisfies the following properties.

- (P1) $P^t \mathbf{1} = \mathbf{1}$ and $P^t f \geq 0$, if $f \geq 0$.
- (P2) $\int P^t f dP_0 = \int f dP_0$, for all $f \in L^2(\mathcal{X}), t \geq 0$.
- (P3) $\mathbf{E}_\chi[f(\theta_{t+h}(\omega)) | \ell_{\leq t}] = P^h F(\omega(t))$, where $F(\chi) := \mathbf{E}_\chi f$, for any $f \in L^1(\Omega), t, h \geq 0, \chi \in \mathcal{X}$.

In the property P3, $\mathbf{E}_\chi[\cdot]$ is the expectation associated with the probability measures $P_\chi, \ell_{\leq t}$ are the σ -algebras generated by events measurable up to time t , and $\theta_t(\omega)(\cdot) := \omega(\cdot + t), t \geq 0$ is the standard shift operator on the path space (Ω, ℓ) .

Moreover, we can define a Markovian measure P on the path space (Ω, ℓ) through

$$P(A) = \int P_\chi(A) P_0(d\chi), \quad A \in \ell \quad (3)$$

and define \mathbf{E} to be the corresponding expectation operator with respect to the measure P . As a direct consequence of (T3) and (P2), we know that P is stationary.

Proposition 2.1. P is invariant under the action of θ_t and $\tau_{\mathbf{x}}$ for any $(t, \mathbf{x}) \in \mathbb{R}^+ \times \mathbb{R}^d$.

Let $L : \mathcal{D}(L) \rightarrow L^2(\mathcal{X})$ be the generator of the semigroup P^t . To establish the central limit theorem for the Markov process associated with P^t , we assume the generator L satisfies the following time relaxation property, also known as the spectral gap condition,

$$-(Lf, f)_{L^2(\mathcal{X})} \geq c_1 \|f\|_{L^2(\mathcal{X})}^2, \text{ where } c_1 > 0. \quad (4)$$

The time relaxation property (4) is equivalent to the exponential decay property

$$\|P^t f\|_{L^2(\mathcal{X})} \leq \exp(-c_1 t) \|f\|_{L^2(\mathcal{X})}, f \in L_0^2(\mathcal{X}). \quad (5)$$

In addition, time relaxation property (4) is equivalent to ρ mixing of the process $X(t)$, $t \geq 0$. Specifically, let $\rho(h) = \sup\{Cor(Y_1, Y_2) : Y_1 \text{ is } \ell_{\geq t+h} \text{ measurable, } Y_2 \text{ is } \ell_{\leq t} \text{ measurable}\}$, where $Cor(Y_1, Y_2)$ is the correlation function. Then, (4) or (5) implies that $\lim_{h \rightarrow \infty} \rho(h) = 0$; see [16, 4]. The time relaxation property (4) (or the exponential decay property (5)) plays an important role in proving the existing of the effective diffusivity. We will numerically investigate this property in Section 5.

2.2. The corrector problem and effective diffusivity

Equipped with the necessary properties and notations, we are ready to study the effective diffusivity of the random flows associated with the passive tracer model (1). First we assume that the random flow $\mathbf{b} = (b_1, \dots, b_d) \in (L^2(\mathcal{X}))^d$ is jointly continuous in (t, \mathbf{x}) , locally Lipschitzian in \mathbf{x} , with finite second moments, and is divergence free. In this paper, we are interested in statistical properties of the solution $\mathbf{X}(t)$, which only requires convergence in law. Therefore, our above assumptions on the velocity field \mathbf{b} are reasonable.

For each fixed realization ω of the environment, we consider the stochastic process generated by the following SDE,

$$\begin{cases} d\mathbf{X}_t^\omega = \mathbf{b}(t, \mathbf{X}_t^\omega, \omega)dt + \sigma d\mathbf{w}_t, \\ \mathbf{X}_0^\omega = 0, \end{cases} \quad (6)$$

where the superscript in \mathbf{X}_t^ω means that it depends on the realization of the environment ω in the random flow \mathbf{b} . Viewed from a particle at any instant of time t , we can define an environment process $\eta : [0, \infty) \times \Omega \rightarrow \mathcal{X}$ as

$$\begin{cases} \eta(t) = \tau_{\mathbf{X}_t^\omega} \omega(t), \\ \eta(0) = \omega(0). \end{cases} \quad (7)$$

In addition, we define $S^t f(\chi) = \mathbf{E}_\chi f(\eta(t))$, $t \geq 0$ for $f \in L^\infty(\mathcal{X})$, where $\eta(t)$ is the environment process given by (7). Then, S^t satisfies the following properties,

Proposition 2.2. (i) $S^t, t \geq 0$ is a strongly continuous, Markov semigroup of contraction on $L^2(\mathcal{X})$.

(ii) $S^t, t \geq 0$ is measure-preserving, that is,

$$\int S^t f dP_0 = \int f dP_0, \quad t \geq 0, \quad f \in L^2(\mathcal{X}). \quad (8)$$

Let $D_1 = \mathcal{D}(L) \cap C_b^2(\mathcal{X})$ and \mathcal{L} denote the generator of the semigroup $S^t, t \geq 0$, i.e.,

$$\mathcal{L}f = Lf + \frac{\sigma^2}{2} \Delta f + \mathbf{b} \cdot \nabla f. \quad (9)$$

One can easily verify the following properties.

Proposition 2.3. (i) D_1 is dense in $L^2(\mathcal{X})$ and is invariant under the semigroup $P^t, t \geq 0$, i.e., $P^t(D_1) \subseteq D_1$ for all $t \geq 0$.

(ii) Assume that the random flow \mathbf{b} is bounded. Then D_1 is invariant under the semigroup $S^t, t \geq 0$, i.e., $S^t(D_1) \subseteq D_1$ for all $t \geq 0$.

Lemma 2.4. From the spectral gap condition (4), we obtain that for any $f \in L_0^2(\mathcal{X})$

$$\|S^t f\|_{L^2(\mathcal{X})} \leq \exp(-c_1 t) \|f\|_{L^2(\mathcal{X})}, \quad \text{where } c_1 > 0. \quad (10)$$

Proof. We first assume \mathbf{b} is bounded and $f \in D_1 \subseteq \mathcal{D}(\mathcal{L})$. Using the spectral gap condition, we have

$$(-\mathcal{L}f, f)_{L_0^2(\mathcal{X})} \geq (-Lf, f)_{L_0^2(\mathcal{X})} \geq c_1 \|f\|_{L_0^2(\mathcal{X})}^2 \quad (11)$$

for all $f \in D_1 \cap L_0^2(\mathcal{X})$. By Proposition 2.3, $S^t f \in D_1, t \geq 0$ for any $f \in D_1$. Consequently,

$$\frac{d}{dt} \|S^t f\|_{L^2(\mathcal{X})}^2 = -2(\mathcal{L}S^t f, S^t f)_{L^2(\mathcal{X})} \leq -2c_1 \|S^t f\|_{L^2(\mathcal{X})}^2, \quad (12)$$

thus

$$\|S^t f\|_{L^2(\mathcal{X})}^2 \leq \exp(-c_1 t) \|f\|_{L^2(\mathcal{X})}^2 \quad \forall t \geq 0 \quad (13)$$

and $f \in D_1 \cap L_0^2(\mathcal{X})$. Then, the statement in (10) is extended to $L_0^2(\mathcal{X})$ by using an approximation argument. Likewise the boundedness of the random flow \mathbf{b} is removed by using another approximation argument. \square

Thanks to Proposition 2.2, we can define

$$\boldsymbol{\psi} = \int_0^\infty S^t \mathbf{b}(t, \mathbf{X}(t), \omega) dt \quad (14)$$

which satisfies the following continuous-type corrector problem

$$\mathcal{L}\boldsymbol{\psi} = -\mathbf{b} \quad (15)$$

where \mathcal{L} is the generator of S^t defined in (9). By solving the corrector problem (15), we are able to define the effective diffusivity. This can be summarized into the following result.

Proposition 2.5. *Let $\mathbf{X}(t)$ be the solution to (1) and $\mathbf{X}_\epsilon(t) \equiv \epsilon\mathbf{X}(t/\epsilon^2)$. For any unit vector $\mathbf{v} \in R^d$, let $\psi_{\mathbf{v}} = \boldsymbol{\psi} \cdot \mathbf{v}$ denote the projection of the vector solution $\boldsymbol{\psi}$ along the direction \mathbf{v} , where $\boldsymbol{\psi}$ is the solution to corrector problem (15). Then, the law of the process $\mathbf{X}_\epsilon(t) \cdot \mathbf{v}$ converges weakly in $C[0, +\infty)$ to a Brownian motion with diffusion coefficient given by*

$$\mathbf{v}^T D^E \mathbf{v} = \frac{\sigma^2}{2} + (-\mathcal{L}\psi_{\mathbf{v}}, \psi_{\mathbf{v}})_{L^2(\mathcal{X})}, \quad (16)$$

where D^E is the effective diffusivity associated with the passive tracer model (1).

The proof of Prop. 2.5 relies on an approximation of the additive functional of an ergodic Markov process by a martingale and applying the central limit theorem to continuous-time Markov process, which is very useful in studying the long-time behavior of a random dynamics; see Lemma 1 of [5] or Theorem of [2]. We shall prove in Theorem 4.3 that the numerical solutions obtained by our Lagrangian numerical scheme recover the definition of the effective diffusivity in (16).

3. Stochastic structure-preserving schemes and related properties

3.1. Derivation of numerical schemes

In this section, we construct numerical schemes for the passive tracer model (6), which is based on an operator splitting method [17]. For each fixed realization $\omega \in \Omega$, we first split the original problem (6) into two sub-problems.

$$d\mathbf{X}_t^\omega = \mathbf{b}(t, \mathbf{X}_t^\omega, \omega)dt, \quad (17)$$

$$d\mathbf{X}_t^\omega = \sigma d\mathbf{w}_t. \quad (18)$$

Let $\mathbf{X}_{n\Delta t}^\omega$ denote the numerical solution of \mathbf{X}_t^ω at time $t = t_n$, $n = 0, 1, 2, \dots$. From time $t = t_n$ to time $t = t_{n+1}$, where $t_{n+1} = t_n + \Delta t$, $t_0 = 0$, assuming the solution $\mathbf{X}_{n\Delta t}^\omega$ is given, we now discuss how to discretize the above two sub-problems (17)-(18), separately.

In the sub-problem (17), the velocity $\mathbf{b}(t, \mathbf{X}(t), \omega)$ is almost surely divergence-free. Thus, we apply a volume-preserving scheme to discretize the velocity. Let $\boldsymbol{\Phi}_{\Delta t}$ denote the numerical integrator associated with the volume-preserving scheme during Δt time and let $\mathbf{D}\boldsymbol{\Phi}_{\Delta t}$ denote the corresponding Jacobian matrix. The volume-preserving property requests $\det(\mathbf{D}\boldsymbol{\Phi}_{\Delta t}) = 1$. We obtain the numerical integrator for the sub-problem (17) as follows,

$$\mathbf{X}_{n+1}^\omega = \boldsymbol{\Phi}_{\Delta t}^{\omega(n\Delta t)}(\mathbf{X}_n^\omega), \quad (19)$$

where the superscript in $\boldsymbol{\Phi}_{\Delta t}^{\omega(n\Delta t)}$ means that the numerical integrator implicitly depends on the realization of \mathbf{b} at different computational times. Suppose \mathbf{b} has bounded first derivatives with respect to \mathbf{x} for almost all ω , it is easy to verify that the volume-preserving integrator $\boldsymbol{\Phi}_{\Delta t}^{\omega(n\Delta t)}$ also has bounded first derivatives for Δt small enough and the n -th step volume-preserving integrator $\boldsymbol{\Phi}_{\Delta t}^{\omega(n\Delta t)}$ is well defined. In addition, we assume that the numerical scheme only relies on the information of \mathbf{X} and \mathbf{b} at the beginning of each computational

time. For instance, to compute \mathbf{X}_{n+1}^ω the numerical scheme only relies on the information of \mathbf{X} and \mathbf{b} (may including high-order derivatives of \mathbf{b}) at $t = t_n$.

Given the numerical integrator $\Phi_{\Delta t}^{\omega(n\Delta t)}$, we define

$$\mathbf{B}_{\Delta t}^{\omega(n\Delta t)}(\mathbf{x}) = \Phi_{\Delta t}^{\omega(n\Delta t)}(\mathbf{x}) - \mathbf{x}. \quad (20)$$

One can easily verify that $\mathbf{B}_{\Delta t}^{\omega(n\Delta t)}$ is an approximation to the exact integrator of the sub-problem (17) as follows,

$$\mathbf{X}_{(n+1)\Delta t}^\omega - \mathbf{X}_{n\Delta t}^\omega = \int_{n\Delta t}^{(n+1)\Delta t} \mathbf{b}(t, \mathbf{X}_t^\omega, \omega) dt. \quad (21)$$

The sub-problem (18) can be approximated easily using the Euler-Maruyama scheme [9].

Finally, we apply the Lie-Trotter splitting method and get the stochastic structure-preserving scheme as follows,

$$\mathbf{X}_{n+1}^\omega = \mathbf{X}_n^\omega + \mathbf{B}_{\Delta t}^{\omega(n\Delta t)}(\mathbf{X}_n^\omega) + \sigma \boldsymbol{\xi}_n, \quad (22)$$

where $\boldsymbol{\xi}_n = (\xi_1, \dots, \xi_d)^T$ is a d -dimensional i.i.d. mean-free Gaussian random vector with $\mathbf{E}\boldsymbol{\xi}_n^T \otimes \boldsymbol{\xi}_n = \Delta t \mathbf{I}_d$, where \mathbf{I}_d is an identity matrix.

The volume-preserving schemes for the sub-problem (17) are implicit in general. Compared with explicit schemes, however, they allow us to choose a relatively larger time step to compute. In practice, we find that few steps of Newton iterations are enough to maintain accurate results. Therefore, the computational cost is controllable. To design adaptive time-stepping method for the passive tracer model (6) is an interesting issue, which will be studied in our future work.

In general, the second-order Strang splitting [17] is more frequently used in developing numerical schemes. In fact, the only difference between the Strang splitting method and the Lie-Trotter splitting method is that the first and last steps are half of the normal step Δt . Thus a more accurate method can be implemented in a very simple way. We skip the details in implementing the Strang splitting scheme here as it is straightforward.

3.2. Some properties of the numerical schemes

In this subsection, we shall prove some properties of the proposed stochastic structure-preserving scheme. Especially, we shall show that some important properties of the random flows are maintained after numerical discretization. Before proceeding to the analysis, we first introduce some notations and assumptions. To emphasize the properties in spatial-domain, for any $f \in L^1(\mathcal{X})$, we use $f^\chi(\mathbf{x})$ to represent $f(\tau_{\mathbf{x}}\chi)$. Moreover, we denote $\mathbf{b}(t, \mathbf{x}, \omega) = \mathbf{b}(\tau_{\mathbf{x}}\omega(t))$, where $\mathbf{b}(\tau_{\mathbf{x}}\omega(t)) \in \mathcal{X}$.

Assumption 3.1. *Suppose the velocity field has certain regularity in the physical space, i.e., $\mathbf{b} \in (C_b^m(\mathcal{X}))^d$ for some $m \geq 2$.*

Assumption 3.2. *$\mathbf{B}_{\Delta t}^\chi(\mathbf{x})$ defined in (20) is a stationary process with respect to \mathbf{x} , i.e., we can write $\mathbf{B}_{\Delta t}^\chi(\mathbf{x}) = \mathbf{B}_{\Delta t}(\tau_{\mathbf{x}}\chi)$.*

Assumption 3.3. $\mathbf{B}_{\Delta t} \in (C_b^m(\mathcal{X}))^d$ provides that $\mathbf{b} \in (C_b^m(\mathcal{X}))^d$ for Δt small enough. And $\|\mathbf{B}_{\Delta t}\|_{C_b^m(\mathcal{X})} = K\|\mathbf{b}\|_{C_b^m(\mathcal{X})}\Delta t$, where K is a constant and does not depend on Δt .

As an analogy to the continuous-time case (7), we define the environment process as viewed from the numerical solution \mathbf{X}_n^ω at different time steps

$$\begin{cases} \eta_n = \tau_{\mathbf{X}_n^\omega} \omega(n\Delta t), \\ \eta_0 = \omega(0). \end{cases} \quad (23)$$

The above environment process induces a probability measure \mathbb{Q}_χ on the space of trajectories $(\tilde{\Omega}, \ell)$, where $\tilde{\Omega} = C([0, \infty) \cap \Delta t\mathbb{Z}; \mathcal{X})$. We denote the corresponding expectation operator as \mathbf{E}_χ . Under this process, we can write $\mathbf{B}_{\Delta t}(\eta_n) = \mathbf{B}_{\Delta t}^{\omega(n\Delta t)}(X_n^\omega)$. In addition, we define

$$S_n f(\chi) = \mathbf{E}_\chi f(\eta_n). \quad (24)$$

We shall prove that, similar to S^t , S_n is a discrete-time Markov semi-group of contraction on $L^2(\mathcal{X})$, and is measure-preserving.

Lemma 3.4. P_0 is an invariant probability measure of η_n , i.e., P_0 is an invariant measure of the Markov semigroup $\{S_n\}$.

Proof. Let $p_\chi^1(\mathbf{x}, \mathbf{y})$ denote the transition probability density of the solution process, which is defined by applying the numerical integrator 22 for one time step. It is known that

$$p_\chi^1(\mathbf{x}, \mathbf{y}) = \frac{1}{(2\pi\sigma^2\Delta t)^{d/2}} \exp\left(-\frac{\|\mathbf{y} - \mathbf{x} - \mathbf{B}_{\Delta t}^\chi(\mathbf{x})\|^2}{2\sigma^2\Delta t}\right) = \frac{1}{(2\pi\sigma^2\Delta t)^{d/2}} \exp\left(-\frac{\|\mathbf{y} - \Phi_{\Delta t}^\chi(\mathbf{x})\|^2}{2\sigma^2\Delta t}\right). \quad (25)$$

Let us define $p_0(\mathbf{x}, \mathbf{y}) = \frac{1}{(2\pi\sigma^2\Delta t)^{d/2}} \exp\left(-\frac{\|\mathbf{y} - \mathbf{x}\|^2}{2\sigma^2\Delta t}\right)$. Then, we can verify that

$$\begin{aligned} \int p_\chi^1(\mathbf{x}, \mathbf{y}) d\mathbf{x} &= \int p_0(\mathbf{x} + \mathbf{B}_{\Delta t}^\chi(\mathbf{x}), \mathbf{y}) d\mathbf{x}, \\ &= \int p_0(\mathbf{z}, \mathbf{y}) \det(\mathbf{D}\Phi_{\Delta t}^\chi)^{-1} d\mathbf{z} = \int p_0(\mathbf{z}, \mathbf{y}) d\mathbf{z} = 1, \quad a.e. \chi, \end{aligned} \quad (26)$$

where we have used the fact $\det(\mathbf{D}\Phi_{\Delta t}^\chi) = 1$. Thus, for all $f \in L^2(\mathcal{X})$, we have

$$\begin{aligned} \int_{\mathcal{X}} S_1 f(\chi) P_0(d\chi) &= \int_{\mathcal{X}} \mathbf{E}_\chi f(\eta_1) P_0(d\chi) = \int_{\mathcal{X}} P_0(d\chi) \int_{R^d} p_\chi^1(\mathbf{0}, \mathbf{y}) \mathbf{E}_\chi f(\tau_{\mathbf{y}} \omega(\Delta t)) d\mathbf{y}, \\ &= \int_{\mathcal{X}} \mathbf{E}_\chi f(\omega(\Delta t)) P_0(d\chi) \int_{R^d} p_{\tau_{-\mathbf{y}}\chi}^1(\mathbf{0}, \mathbf{y}) d\mathbf{y}, \\ &= \int_{\mathcal{X}} \mathbf{E}_\chi f(\omega(\Delta t)) P_0(d\chi) \int_{R^d} p_\chi^1(-\mathbf{y}, \mathbf{0}) d\mathbf{y}, \end{aligned} \quad (27)$$

where we have used the fact that $p_{\tau_{\mathbf{x}}\chi}^n(\mathbf{y}, \mathbf{z}) = p_\chi^n(\mathbf{y} + \mathbf{x}, \mathbf{z} + \mathbf{x})$. Follow from 26, we have $\mathbf{E}S_1 f = \mathbf{E}P^{\Delta t} f = \mathbf{E}f$, where $P^{\Delta t}$ is measure-preserving by property (P2) in Section 2.1. Similar argument shows that $\mathbf{E}S_n f = \mathbf{E}S_{n-1} f$ for all n . Thus, S_n is measure-preserving. \square

The following lemma will be very useful in our analysis.

Lemma 3.5. *For any $\mathbf{y} \in R^d$ and $f \in L^2(\mathcal{X})$, we have that*

$$\mathbf{E}f(\tau_{\mathbf{y}}\eta_n) = \mathbf{E}f(\eta_{n-1}) = \mathbf{E}f. \quad (28)$$

Moreover,

$$\mathbf{E}f(\eta_{n+1}) = \mathbf{E}f(\tau_{\mathbf{X}_n^\omega + \mathbf{b}_{\Delta t}(\eta_n)}\omega((n+1)\Delta t)) = \mathbf{E}f. \quad (29)$$

Proof. We prove the above equations through direct calculations. For the equation (28),

$$\begin{aligned} \mathbf{E}f(\tau_{\mathbf{y}}\eta_n) &= \mathbf{E}\mathbf{E}_{\eta_{n-1}}f(\tau_{\mathbf{y}}\tilde{\eta}_1) = \int_{\mathcal{X}} P_0(d\chi) \int_{R^d} p_{\eta_{n-1}}^1(\mathbf{0}, \mathbf{z}) \mathbf{E}_{\eta_{n-1}}f(\tau_{\mathbf{y}+\mathbf{z}}\omega(\Delta t)) d\mathbf{z}, \\ &= \int_{\mathcal{X}} \mathbf{E}_{\eta_{n-1}}f(\omega(\Delta t)) P_0(d\chi) \int_{R^d} p_{\tau_{-\mathbf{y}-\mathbf{z}}\eta_{n-1}}^1(\mathbf{0}, \mathbf{z}) d\mathbf{z}, \\ &= \int_{\mathcal{X}} \mathbf{E}_{\eta_{n-1}}f(\omega(\Delta t)) P_0(d\chi) \int_{R^d} p_{\eta_{n-1}}^1(-\mathbf{y} - \mathbf{z}, -\mathbf{y}) d\mathbf{z}, \\ &= \int_{\mathcal{X}} \mathbf{E}_{\eta_{n-1}}f(\omega(\Delta t)) P_0(d\chi) = \int_{\mathcal{X}} f(\eta_{n-1}) P_0(d\chi), \end{aligned} \quad (30)$$

where $\{\tilde{\eta}_1\}$ is as defined in 23 but with initial condition $\tilde{\eta}_0 = \eta_{n-1}$. For the equation (29), let $\mathbf{Y}_n^\omega = \mathbf{X}_n^\omega + \mathbf{B}_{\Delta t}(\eta_n) = \mathbf{X}_{n+1}^\omega - \sigma\xi_n$. Then, we have

$$\begin{aligned} \mathbf{E}f(\eta_{n+1}) &= \mathbf{E}\mathbf{E}_{\eta_n}f(\tau_{\mathbf{Y}_n^\omega + \sigma\xi_n}\omega(\Delta t)) = \int_{\mathcal{X}} P_0(d\chi) \int_{R^d} p_0(\mathbf{0}, \mathbf{z}) \mathbf{E}_{\eta_n}f(\tau_{\mathbf{z}}\tau_{\mathbf{Y}_n^\omega}\omega(\Delta t)) d\mathbf{z}, \\ &= \int_{\mathcal{X}} \mathbf{E}_{\eta_n}f(\tau_{\mathbf{Y}_n^\omega}\omega(\Delta t)) P_0(d\chi) \int_{R^d} p_0(\mathbf{0}, \mathbf{z}) d\mathbf{z}, \\ &= \mathbf{E}f(\tau_{\mathbf{X}_n^\omega + \mathbf{b}_{\Delta t}(\eta_n)}\omega((n+1)\Delta t)). \end{aligned} \quad (31)$$

□

Equipped with these preparations, we can state the main results. The first result is that the operator S_n defined in (24) is a contractive map on $L^2(\mathcal{X})$.

Theorem 3.6. *S_n has the property that*

$$\|S_n f\|_{L^2(\mathcal{X})} \leq \exp(-c_1 n \Delta t) \|f\|_{L^2(\mathcal{X})}, \quad (32)$$

for all $f \in L_0^2(\mathcal{X})$.

Proof. We first study the case when $n = 1$. The key observation is that

$$\begin{aligned}
& \int_{\mathcal{X}} S_1 f(\chi) \cdot S_1 f(\chi) P_0(d\chi) = \int_{\mathcal{X}} \mathbf{E}_{\chi} f(\eta_1) \cdot \mathbf{E}_{\chi} f(\eta_1) P_0(d\chi), \\
& = \int_{\mathcal{X}} P_0(d\chi) \int_{R^d} p_{\chi}^1(\mathbf{0}, \mathbf{y}) \mathbf{E}_{\chi} f(\tau_{\mathbf{y}} \omega(\Delta t)) d\mathbf{y} \cdot \int_{R^d} p_{\chi}^1(\mathbf{0}, \mathbf{y}) \mathbf{E}_{\chi} f(\tau_{\mathbf{y}} \omega(\Delta t)) d\mathbf{y}, \\
& \leq \int_{\mathcal{X}} P_0(d\chi) \int_{R^d} p_{\chi}^1(\mathbf{0}, \mathbf{y}) \mathbf{E}_{\chi} f(\tau_{\mathbf{y}} \omega(\Delta t)) \cdot \mathbf{E}_{\chi} f(\tau_{\mathbf{y}} \omega(\Delta t)) d\mathbf{y}, \\
& = \int_{\mathcal{X}} \mathbf{E}_{\chi} f(\omega(\Delta t)) \cdot \mathbf{E}_{\chi} f(\omega(\Delta t)) P_0(d\chi) \int_{R^d} p_{\chi}^1(-\mathbf{y}, \mathbf{0}) d\mathbf{y}, \\
& = \int_{\mathcal{X}} P^{\Delta t} f(\chi) \cdot P^{\Delta t} f(\chi) P_0(d\chi), \tag{33}
\end{aligned}$$

where $P^{\Delta t}$ is a strongly continuous Markov semigroup on $L^2(\mathcal{X})$. In the third line of (33), we use the fact that $p_{\chi}^1(\mathbf{0}, \mathbf{y})$ is a probability density function so we can easily get the result by Cauchy-Schwarz inequality. Therefore, we obtain

$$\|S_1 f\|_{L^2(\mathcal{X})} \leq \|P^{\Delta t} f\|_{L^2(\mathcal{X})} \leq \exp(-c_1 \Delta t) \|f\|_{L^2(\mathcal{X})}, \tag{34}$$

where the exponential decay property (5) is applied. The assertion in (32) can be obtained if we repeat to use the above property n times. \square

Next, we define $\bar{\mathbf{B}}_{\Delta t} = \mathbf{E} \mathbf{B}_{\Delta t}$ and $\tilde{\mathbf{B}}_{\Delta t} = \mathbf{B}_{\Delta t} - \bar{\mathbf{B}}_{\Delta t}$. We aim to get some estimates for the operator $\bar{\mathbf{B}}_{\Delta t}$ and the numerical solution $\mathbf{E} \mathbf{X}_n^{\omega}$, which are important in our convergence analysis for the effective diffusivity.

Theorem 3.7. *If we choose a second-order numerical scheme in computing (19), then $\bar{\mathbf{B}}_{\Delta t}$ is of order $(\Delta t)^2$. In addition, $\mathbf{E} \mathbf{X}_n^{\omega} - n \bar{\mathbf{B}}_{\Delta t}$ is bounded.*

Proof. By using a second-order numerical scheme to compute (19), we have

$$\mathbf{E} \mathbf{B}_{\Delta t} = \mathbf{E} \int_0^{\Delta t} \mathbf{b}(t, X_t^{\omega}, \cdot) dt + O(\Delta t)^2 = \mathbf{E} \int_0^{\Delta t} \mathbf{b}(\eta_t^0) dt + O(\Delta t)^2, \tag{35}$$

where η_t^0 is the environment process defined in 7 with $\sigma = 0$. Because when we define $\mathbf{B}_{\Delta t}$, we only consider the sub-problem (17). Recall the fact that S^t is measure-preserving, we get

$$\mathbf{E} \int_0^{\Delta t} \mathbf{b}(\eta_t^0) dt = \int_0^{\Delta t} \int_{\mathcal{X}} \mathbf{E}_{\chi} \mathbf{b}(\eta_t^0) dP_0(\chi) dt = \int_0^{\Delta t} \mathbf{E} S^t \mathbf{b} dt = \int_0^{\Delta t} \mathbf{E} \mathbf{b} dt = 0. \tag{36}$$

Therefore, $\mathbf{E} \mathbf{B}_{\Delta t}$ is of order $(\Delta t)^2$. Moreover, from the numerical scheme (22) we have

$$\mathbf{E} \mathbf{X}_n^{\omega} = \mathbf{E} \mathbf{X}_{n-1}^{\omega} + \mathbf{E} \mathbf{B}_{\Delta t}^{\omega(n\Delta t)}(\mathbf{X}_n^{\omega}) = \mathbf{E} \mathbf{X}_0^{\omega} + \sum_{i=0}^{n-1} \mathbf{E} S_i \mathbf{B}_{\Delta t} = \mathbf{E} \mathbf{X}_0^{\omega} + \sum_{i=0}^{n-1} \mathbf{E} S_i \tilde{\mathbf{B}}_{\Delta t} + n \bar{\mathbf{B}}_{\Delta t}. \tag{37}$$

According to 32, we can easily verify that $\sum_{i=0}^{n-1} S_i \tilde{\mathbf{B}}_{\Delta t}$ is bounded in $L^2(\mathcal{X})$, which implies $|\sum_{i=0}^{n-1} \mathbf{E} S_i \tilde{\mathbf{B}}_{\Delta t}| < \infty$. Thus, we complete the proof. \square

The corrector problem (15) plays an important role in defining the effective diffusivity for the random flow. To study the property of the numerical solutions, we will define a discrete-type corrector problem and study the property of the solution.

Theorem 3.8. *Let us define $\boldsymbol{\psi}_{\Delta t} = \sum_{i=0}^{\infty} S_i \tilde{\mathbf{B}}_{\Delta t}$. Then, $\boldsymbol{\psi}_{\Delta t}$ is the unique solution in $(L_0^2(\mathcal{X}))^d$ of the discrete-type corrector problem as follows*

$$(S_1 - I)\boldsymbol{\psi}_{\Delta t} = -\tilde{\mathbf{B}}_{\Delta t}. \quad (38)$$

Proof. The formulation of $\boldsymbol{\psi}_{\Delta t}$ solves the discrete-type corrector problem 38 can be easily verified through simple calculations, i.e.,

$$(S_1 - I)\boldsymbol{\psi}_{\Delta t} = \sum_{i=1}^{\infty} S_i \tilde{\mathbf{B}}_{\Delta t} - \sum_{i=0}^{\infty} S_i \tilde{\mathbf{B}}_{\Delta t} = -\tilde{\mathbf{B}}_{\Delta t}. \quad (39)$$

$E\boldsymbol{\psi}_{\Delta t} = 0$ is a straight forward result from the formulation of $\boldsymbol{\psi}_{\Delta t}$. The uniqueness comes from Theorem 3.6. Suppose the equation (38) has two different solutions $\boldsymbol{\psi}_1, \boldsymbol{\psi}_2 \in L_0^2(\mathcal{X})$, we have that $(S_1 - I)(\boldsymbol{\psi}_1 - \boldsymbol{\psi}_2) = 0$, then

$$\|\boldsymbol{\psi}_1 - \boldsymbol{\psi}_2\|_{L^2(\mathcal{X})} = \|S_1(\boldsymbol{\psi}_1 - \boldsymbol{\psi}_2)\|_{L^2(\mathcal{X})} \leq \exp(-c_1 \Delta t) \|\boldsymbol{\psi}_1 - \boldsymbol{\psi}_2\|_{L^2(\mathcal{X})},$$

which implies that $\boldsymbol{\psi}_1 - \boldsymbol{\psi}_2 = 0$. Thus, the uniqueness of the equation 38 is proved. \square

Remark 3.1. The discrete-type corrector problem 38 is equivalent to the equation

$$\mathbf{E}[\boldsymbol{\psi}_{\Delta t}^{\omega(i\Delta t)}(\mathbf{X}_i^\omega) | \mathbf{X}_{i-1}^\omega] - \boldsymbol{\psi}_{\Delta t}^{\omega((i-1)\Delta t)}(\mathbf{X}_{i-1}^\omega) = -\tilde{\mathbf{B}}_{\Delta t}^{\omega(i\Delta t)}(\mathbf{X}_{i-1}^\omega). \quad (40)$$

This can be seen by replacing χ with η_{n-1} in the definition of S_1 .

Finally, we study the regularity of the solution of the discrete-type corrector problem (38). The following result is based on the regularity assumption on the velocity field \mathbf{b} . We are interested in statistical properties of the solution $\mathbf{X}(t)$, which only requires convergence in law. Thus, we can choose smooth realizations of the velocity field \mathbf{b} .

Theorem 3.9. *Suppose $\mathbf{b} \in (C_b^m(\mathcal{X}))^d$, then $\boldsymbol{\psi}_{\Delta t}$ is in $(H^m(\mathcal{X}))^d$.*

Proof. First we prove that, under the assumption $\mathbf{b} \in (C_b^m(\mathcal{X}))^d$ for $m \geq 1$, we have that for any $f \in L^2(\mathcal{X})$, $S_1 f \in H^1(\mathcal{X})$. Since

$$\begin{aligned} S_1 f(\tau_{\mathbf{x}}\chi) &= \int_{R^d} p_{\tau_{\mathbf{x}}\chi}^1(\mathbf{0}, \mathbf{y}) P^{\Delta t} f(\tau_{\mathbf{x}+\mathbf{y}}\chi) d\mathbf{y} = \int_{R^d} p_{\chi}^1(\mathbf{x}, \mathbf{x} + \mathbf{y}) P^{\Delta t} f(\tau_{\mathbf{x}+\mathbf{y}}\chi) d\mathbf{y}, \\ &= \int_{R^d} p_{\chi}^1(\mathbf{x}, \mathbf{y}) P^{\Delta t} f(\tau_{\mathbf{y}}\chi) d\mathbf{y}, \end{aligned} \quad (41)$$

where $p_{\chi}^1(\mathbf{x}, \mathbf{y})$ is the transition probability density defined in (25). Notice that

$$\mathbf{D}_{\mathbf{x}} p_{\chi}^1(\mathbf{x}, \mathbf{y}) = 2(I + \mathbf{D}\mathbf{B}_{\Delta t}^{\chi}(\mathbf{x}))(\mathbf{y} - \mathbf{x} - \mathbf{B}_{\Delta t}^{\chi}(\mathbf{x})) p_{\chi}^1(\mathbf{x}, \mathbf{y}), \quad (42)$$

and $\mathbf{B}_{\Delta t} \in (C_b^m(\mathcal{X}))^d$, we can obtain that $\int_{R^d} (\mathbf{y} - \mathbf{x} - \mathbf{B}_{\Delta t}^x(\mathbf{x}))^2 p_\chi^1(\mathbf{x}, \mathbf{y}) d\mathbf{x}$ is uniformly bounded for almost all χ . This concludes that

$$\int_{R^d} \mathbf{D}_x p_\chi^1(\mathbf{x}, \mathbf{y}) P^{\Delta t} f(\tau_y \chi) d\mathbf{y} \in L^2(\mathcal{X}). \quad (43)$$

The statement (43) implies that $\mathbf{D}S_1 f \in L^2(\mathcal{X})$ by the dominant convergence theorem. Thus $S_1 f \in H^1(\mathcal{X})$. According to the definition of the discrete-type corrector problem (38), $\psi_{\Delta t}$ satisfies

$$\psi_{\Delta t} = S_1 \psi_{\Delta t} + \tilde{\mathbf{B}}_{\Delta t}. \quad (44)$$

Therefore, we obtain that $\psi_{\Delta t} \in (H^1(\mathcal{X}))^d$. Moreover, noticing that

$$\begin{aligned} \mathbf{D}S_1 f(\chi) &= \int_{R^d} \mathbf{D}_x p_\chi^1(\mathbf{0}, \mathbf{y}) P^{\Delta t} f(\tau_y \chi) d\mathbf{y}, \\ &= \int_{R^d} 2(I + \mathbf{D}\mathbf{B}_{\Delta t}^x(0))(\mathbf{y} - \mathbf{0} - \mathbf{B}_{\Delta t}^x(0)) p_\chi^1(\mathbf{x}, \mathbf{y}) P^{\Delta t} f(\tau_y \chi) d\mathbf{y}, \\ &= 2(I + \mathbf{D}\mathbf{B}_{\Delta t}^x(0)) \int_{R^d} -\mathbf{D}_y p_\chi^1(\mathbf{0}, \mathbf{y}) P^{\Delta t} f(\tau_y \chi) d\mathbf{y}, \\ &= 2(I + \mathbf{D}\mathbf{B}_{\Delta t}^x(0)) \int_{R^d} p_\chi^1(\mathbf{0}, \mathbf{y}) \mathbf{D}_y P^{\Delta t} f(\tau_y \chi) d\mathbf{y}, \\ &= 2(I + \mathbf{D}\mathbf{B}_{\Delta t}^x(0)) S_1 \mathbf{D}f(\chi). \end{aligned} \quad (45)$$

We arrive that

$$\mathbf{D}\psi_{\Delta t} = 2(I + \mathbf{D}\mathbf{B}_{\Delta t}) S_1 \mathbf{D}\psi_{\Delta t} + \mathbf{D}\tilde{\mathbf{B}}_{\Delta t}. \quad (46)$$

Similar argument shows that $\mathbf{D}\psi_{\Delta t} \in (H^1(\mathcal{X}))^{d \times d}$. Doing this argument recursively shows that $\psi_{\Delta t}$ is in $(H^m(\mathcal{X}))^d$. \square

4. Convergence analysis

In this section, we shall prove the convergence rate of our stochastic structure-preserving scheme in computing effective diffusivity. The convergence analysis is based on a probabilistic approach, which allows us to get rid of the exponential growth factor in the error estimate.

4.1. Convergence of the discrete-type corrector problem to the continuous one

We first show that, if Δt is small enough, $S^{\Delta t}$ will converge to S_1 . Moreover, the following statement holds.

Lemma 4.1. *If f is a globally Lipschitz function with respect to \mathbf{x} , then we have*

$$\|S_n f - S^{n\Delta t} f\|_{L^2(\mathcal{X})} \leq c_2 L(\Delta t)^2, \quad (47)$$

where L is the Lipschitz constant for f and c_2 depends only on the computational time $T = n\Delta t$.

Proof. First we have that $(S_n - S^{n\Delta t})f(\chi) = \mathbf{E}_\chi(f(\eta_n) - f(\eta(n\Delta t)))$. This implies that

$$(S_n - S^{n\Delta t})f(\chi) \leq \mathbf{E}_\chi |\mathbf{X}_n^\omega - \mathbf{X}_{n\Delta t}^\omega| L. \quad (48)$$

A basic comparison with Euler-Maruyama method [9] shows that $\mathbf{E}_\chi |X_n^\omega - X_{n\Delta t}^\omega| < c_2(\Delta t)^2$ for all χ with the bounded assumption for \mathbf{b} ; see Asm. 3.1. \square

Then, we show that under certain conditions the discrete-type corrector problem converges to the continuous one, which facilitates the convergence analysis of our numerical method in computing the effective diffusivity for random flows.

Theorem 4.2. *The solution $\psi_{\Delta t}$ converges to the solution ψ of the continuous-type corrector problem defined in (14) in $L^2(\mathcal{X})$, as $\Delta t \rightarrow 0$.*

Proof. For any $\epsilon > 0$, using the exponential decay properties of S^t and S_n , we first take T big enough such that the following inequalities hold

$$\left\| \int_{T-\Delta t}^{\infty} S^t \mathbf{b} dt \right\|_{L^2(\mathcal{X})} < \epsilon, \quad \text{and} \quad \left\| \sum_{n=[T/\Delta t]-1}^{\infty} S_n \tilde{\mathbf{B}}_{\Delta t} \right\|_{L^2(\mathcal{X})} \approx \frac{1}{c_1} \exp(-c_1 T) < \epsilon. \quad (49)$$

Next we estimate the error between $\sum_{n=0}^{N-1} S_n \tilde{\mathbf{B}}_{\Delta t}$ and $\int_0^{N\Delta t} S^t \mathbf{b} dt$ for $N \leq T/\Delta t$. We know that

$$\left\| \int_0^{N\Delta t} S^t \mathbf{b} dt - \sum_{n=0}^{N-1} S^{n\Delta t} \mathbf{b} \Delta t \right\|_{L^2(\mathcal{X})} \leq C_1 \Delta t \quad (50)$$

due to the strongly continuity of S^t (see Prop. 2.2) and

$$\begin{aligned} \left\| \sum_{n=0}^{N-1} S_n \tilde{\mathbf{B}}_{\Delta t} - \sum_{n=0}^{N-1} S^{n\Delta t} \mathbf{b} \Delta t \right\|_{L^2(\mathcal{X})} &\leq \left\| \sum_{n=0}^{N-1} S_n \tilde{\mathbf{B}}_{\Delta t} - \sum_{n=0}^{N-1} S_n \mathbf{b} \Delta t \right\|_{L^2(\mathcal{X})} \\ &\quad + \left\| \sum_{n=0}^{N-1} S_n \mathbf{b} \Delta t - \sum_{n=0}^{N-1} S^{n\Delta t} \mathbf{b} \Delta t \right\|_{L^2(\mathcal{X})}. \end{aligned} \quad (51)$$

Since local truncation error of the numerical scheme (19) is at least second order, we have $\|\tilde{\mathbf{B}}_{\Delta t} - \mathbf{b}\|_{L^2(\mathcal{X})} \leq O(\Delta t)^2$. The lemma 4.1 implies $\|(S_n - S^{n\Delta t})\mathbf{b}\Delta t\|_{L^2(\mathcal{X})} \leq O(\Delta t)^2$ for all $n \leq N$. This gives the estimate

$$\left\| \sum_{n=0}^{N-1} S_n \tilde{\mathbf{B}}_{\Delta t} - \sum_{n=0}^{N-1} S^{n\Delta t} \mathbf{b} \Delta t \right\|_{L^2(\mathcal{X})} \leq c_2 N (\Delta t)^2 \leq c_2 T \Delta t. \quad (52)$$

Finally, we take $\Delta t \leq \epsilon/(c_2 T)$ and obtain

$$\left\| \int_0^{\infty} S^t \mathbf{b} dt - \sum_{n=0}^{\infty} S_n \tilde{\mathbf{B}}_{\Delta t} \right\|_{L^2(\mathcal{X})} \leq 3\epsilon. \quad (53)$$

We prove the assertion of the Theorem. \square

Remark 4.1. The constant c_2 in Lemma 4.1 is actually exponentially depends on T , i.e., $c_2 = \exp(c_3 T)$. To balance each value of ϵ , we have $K \exp(-c_1 T) = \exp(c_3 T) T \Delta t$, which requires $T \approx -1/(c_1 + c_3) \log \Delta t$ and $\epsilon \approx C \Delta t^{\frac{c_1}{c_1 + c_3}}$.

4.2. Convergence of the numerical method in computing effective diffusivity

Now we are in a position to show the main results of our paper. We prove that the effective diffusivity obtained by our numerical method converges to the exact one defined in (16).

Theorem 4.3. *Let \mathbf{X}_n^ω , $n = 0, 1, \dots$ be the numerical solution of the stochastic structure-preserving scheme (22) and Δt be the time-step. Let $\bar{\mathbf{X}}_n^\omega = \mathbf{X}_n^\omega - n\bar{\mathbf{B}}_{\Delta t}$. We have the convergence estimate of the numerical method in computing effective diffusivity as*

$$\frac{\mathbf{E}\bar{\mathbf{X}}_n^\omega \otimes \bar{\mathbf{X}}_n^\omega}{n\Delta t} = \sigma^2 \mathbf{I}_d + 2\mathbf{S} \int_{\mathcal{X}} \boldsymbol{\psi} \otimes \mathbf{b} dP_0 + \rho(\Delta t) + O\left(\frac{1}{n\Delta t}\right), \quad (54)$$

where $\rho(\Delta t)$ is a function satisfying $\lim_{\Delta t \rightarrow 0} \rho(\Delta t) = 0$ and independent of the computational time T . The \mathbf{S} represents the symmetrization operator on a matrix, i.e., $\mathbf{S}\mathbf{A} = \frac{\mathbf{A} + \mathbf{A}^T}{2}$.

Proof. First of all, from direct computations we can obtain that

$$\begin{aligned} \mathbf{E}\bar{\mathbf{X}}_n^\omega \otimes \bar{\mathbf{X}}_n^\omega &= \mathbf{E}(\bar{\mathbf{X}}_{n-1}^\omega + \tilde{\mathbf{B}}_{\Delta t}^{\omega((n-1)\Delta t)}(\mathbf{X}_{n-1}^\omega) + \sigma \boldsymbol{\xi}_{n-1}) \otimes (\bar{\mathbf{X}}_{n-1}^\omega + \tilde{\mathbf{B}}_{\Delta t}^{\omega((n-1)\Delta t)}(\mathbf{X}_{n-1}^\omega) + \sigma \boldsymbol{\xi}_{n-1}), \\ &= \mathbf{E}\bar{\mathbf{X}}_{n-1}^\omega \otimes \bar{\mathbf{X}}_{n-1}^\omega + \sigma^2 \mathbf{I}_d \Delta t + 2\mathbf{S}\mathbf{E}\bar{\mathbf{X}}_{n-1}^\omega \otimes \tilde{\mathbf{B}}_{\Delta t}^{\omega((n-1)\Delta t)}(\mathbf{X}_{n-1}^\omega) + \mathbf{E}\tilde{\mathbf{B}}_{\Delta t}^{\omega((n-1)\Delta t)}(\bar{\mathbf{X}}_{n-1}^\omega) \otimes \tilde{\mathbf{B}}_{\Delta t}^{\omega((n-1)\Delta t)}(\mathbf{X}_{n-1}^\omega), \\ &= \mathbf{E}\bar{\mathbf{X}}_0^\omega \otimes \bar{\mathbf{X}}_0^\omega + \sigma^2 \mathbf{I}_d n \Delta t + 2 \sum_{i=1}^n \mathbf{S}\mathbf{E}\bar{\mathbf{X}}_{i-1}^\omega \otimes \tilde{\mathbf{B}}_{\Delta t}^{\omega((i-1)\Delta t)}(\bar{\mathbf{X}}_{i-1}^\omega) + \sum_{i=1}^n \mathbf{E}\tilde{\mathbf{B}}_{\Delta t}^{\omega((i-1)\Delta t)}(\mathbf{X}_{i-1}^\omega) \otimes \tilde{\mathbf{B}}_{\Delta t}^{\omega((i-1)\Delta t)}(\mathbf{X}_{i-1}^\omega), \end{aligned} \quad (55)$$

where we use the condition that $\boldsymbol{\xi}_{n-1}$ is independent with $\bar{\mathbf{X}}_{n-1}^\omega$ and \mathbf{S} is the symmetrization operator. Notice that $\frac{\mathbf{E}\bar{\mathbf{X}}_0^\omega \otimes \bar{\mathbf{X}}_0^\omega}{n\Delta t}$ vanishes as $n \rightarrow +\infty$ and $\frac{\sigma^2 \mathbf{I}_d n \Delta t}{n\Delta t} = \sigma^2 \mathbf{I}_d$. We main need to estimate the third term and fourth term on the right hand side of (55), separately.

For the third term on the right hand side of (55), using the property of the discrete-type corrector problem (40), we obtain that

$$\begin{aligned} & - \sum_{i=1}^n \mathbf{E}\bar{\mathbf{X}}_{i-1}^\omega \otimes \tilde{\mathbf{B}}_{\Delta t}^{\omega(i\Delta t)}(\mathbf{X}_{i-1}^\omega) = \sum_{i=0}^{n-1} \mathbf{E}\bar{\mathbf{X}}_{i-1}^\omega \otimes (\mathbf{E}[\boldsymbol{\psi}_{\Delta t}^{\omega(i\Delta t)}(\mathbf{X}_i^\omega) | \mathbf{X}_{i-1}^\omega] - \boldsymbol{\psi}_{\Delta t}^{\omega((i-1)\Delta t)}(\mathbf{X}_{i-1}^\omega)), \\ &= \sum_{i=1}^n \mathbf{E}\bar{\mathbf{X}}_{i-1}^\omega \otimes (\boldsymbol{\psi}_{\Delta t}^{\omega(i\Delta t)}(\mathbf{X}_i^\omega) - \boldsymbol{\psi}_{\Delta t}^{\omega((i-1)\Delta t)}(\mathbf{X}_{i-1}^\omega)), \\ &= \sum_{i=1}^n \mathbf{E}(\bar{\mathbf{X}}_{i-1}^\omega - \bar{\mathbf{X}}_i^\omega) \otimes \boldsymbol{\psi}_{\Delta t}^{\omega(i)}(\mathbf{X}_i^\omega) + \bar{\mathbf{X}}_0^\omega \otimes \boldsymbol{\psi}_{\Delta t}^{\omega(0)}(\mathbf{X}_0^\omega) - \mathbf{E}\bar{\mathbf{X}}_n^\omega \otimes \boldsymbol{\psi}_{\Delta t}^{\omega(n\Delta t)}(\mathbf{X}_n^\omega), \\ &= \sum_{i=1}^n -\mathbf{E}(\tilde{\mathbf{B}}_{\Delta t}^{\omega((i-1)\Delta t)}(\mathbf{X}_{i-1}^\omega) + \sigma \boldsymbol{\xi}_{i-1}) \otimes \boldsymbol{\psi}_{\Delta t}^{\omega(i\Delta t)}(\mathbf{X}_i^\omega) + \bar{\mathbf{X}}_0^\omega \otimes \boldsymbol{\psi}_{\Delta t}^{\omega(0)}(\mathbf{X}_0^\omega) - \mathbf{E}\bar{\mathbf{X}}_n^\omega \otimes \boldsymbol{\psi}_{\Delta t}^{\omega(n\Delta t)}(\mathbf{X}_n^\omega). \end{aligned} \quad (56)$$

Notice that

$$2\mathbf{E}(\bar{\mathbf{X}}_n^\omega)_i (\boldsymbol{\psi}_{\Delta t}^{\omega(n\Delta t)}(\bar{\mathbf{X}}_n^\omega))_j \leq \epsilon \mathbf{E}[(\bar{\mathbf{X}}_n^\omega)_i]^2 + \epsilon^{-1} \mathbf{E}[(\boldsymbol{\psi}_{\Delta t}^{\omega(n\Delta t)}(\mathbf{X}_n^\omega))_j]^2, \quad 1 \leq i, j \leq d. \quad (57)$$

We choose ϵ small enough, then move $\epsilon \mathbf{E}[(\bar{\mathbf{X}}_n^\omega)_i]^2$ to the left hand side of the equation 55, then the remaining terms on the right hand side are all bounded due to the ergodicity of $\bar{\mathbf{X}}_n^\omega$. Thus we can obtain that $\frac{1}{n} \mathbf{E} \|\bar{\mathbf{X}}_n^\omega\|^2$ is bounded by the ergodicity of $\bar{\mathbf{X}}_n^\omega$. Thus

$$\frac{1}{n} \mathbf{E} \bar{\mathbf{X}}_n^\omega \otimes \boldsymbol{\psi}_{\Delta t}^{\omega(n\Delta t)}(\mathbf{X}_n^\omega) \rightarrow 0, \quad \text{as } n \rightarrow \infty. \quad (58)$$

Using the property that S_i is measure-preserving 3.4 and Theorem 3.7, we get

$$\frac{1}{n} \sum_{i=0}^{n-1} \mathbf{E} \tilde{\mathbf{B}}_{\Delta t}^{\omega(i\Delta t)}(\mathbf{X}_i^\omega) \otimes \tilde{\mathbf{B}}_{\Delta t}^{\omega(i\Delta t)}(\mathbf{X}_i^\omega) = \frac{1}{n} n \mathbf{E} \tilde{\mathbf{B}}_{\Delta t} \otimes \tilde{\mathbf{B}}_{\Delta t} = O(\Delta t)^2. \quad (59)$$

For the leftmost term on the right hand side of the last equation (56), we have

$$\begin{aligned} & \mathbf{E}(\tilde{\mathbf{B}}_{\Delta t}^{\omega((i-1)\Delta t)}(\mathbf{X}_{i-1}^\omega) + \sigma \boldsymbol{\xi}_{i-1}) \otimes \boldsymbol{\psi}_{\Delta t}^{\omega(i\Delta t)}(\mathbf{X}_i^\omega), \\ &= \mathbf{E}(\tilde{\mathbf{B}}_{\Delta t}^{\omega((i-1)\Delta t)}(\mathbf{X}_{i-1}^\omega) + \sigma \boldsymbol{\xi}_{i-1}) \otimes \boldsymbol{\psi}_{\Delta t}^{\omega(i\Delta t)}(\mathbf{X}_{i-1}^\omega + \mathbf{B}_{\Delta t}^\omega(\mathbf{X}_{i-1}^\omega) + \sigma \boldsymbol{\xi}_{i-1}), \\ &= \mathbf{E} \tilde{\mathbf{B}}_{\Delta t}^{\omega((i-1)\Delta t)}(\mathbf{X}_{i-1}^\omega) \otimes \boldsymbol{\psi}_{\Delta t}^{\omega(i\Delta t)}(\mathbf{X}_i^\omega) + \mathbf{E} \sigma \boldsymbol{\xi}_{i-1} \otimes \boldsymbol{\psi}_{\Delta t}^{\omega(i\Delta t)}(\mathbf{X}_{i-1}^\omega + \mathbf{B}_{\Delta t}^{\omega((i-1)\Delta t)}(\mathbf{X}_{i-1}^\omega) + \sigma \boldsymbol{\xi}_{i-1}). \end{aligned} \quad (60)$$

By the Fubini's theorem, we know that the second term on the last line of (60) vanishes. Specifically, we can compute it as follows,

$$\begin{aligned} & \mathbf{E} \sigma \boldsymbol{\xi}_{i-1} \otimes \boldsymbol{\psi}_{\Delta t}^{\omega(i\Delta t)}(\mathbf{X}_{i-1}^\omega + \mathbf{b}_{\Delta t}^{\omega((i-1)\Delta t)}(\mathbf{X}_{i-1}^\omega) + \sigma \boldsymbol{\xi}_{i-1}), \\ &= \int_{\mathcal{X}} \int_{R^d} p_0(\mathbf{0}, \mathbf{y}) \sigma \mathbf{y} \otimes \boldsymbol{\psi}_{\Delta t}(\tau_{\sigma \mathbf{y}} \tau_{\mathbf{X}_{i-1}^\omega + \mathbf{b}_{\Delta t}(\eta_{i-1})} \omega(i\Delta t)) d\mathbf{y} P_0(d\chi), \\ &= \int_{R^d} p_0(\mathbf{0}, \mathbf{y}) \sigma \mathbf{y} \otimes \int_{\mathcal{X}} \boldsymbol{\psi}_{\Delta t}(\tau_{\sigma \mathbf{y}} \tau_{\mathbf{X}_{i-1}^\omega + \mathbf{b}_{\Delta t}(\eta_{i-1})} \omega(i\Delta t)) P_0(d\chi) d\mathbf{y}, \\ &= \int_{R^d} p_0(\mathbf{0}, \mathbf{y}) \sigma \mathbf{y} \otimes \int_{\mathcal{X}} \boldsymbol{\psi}_{\Delta t}(\tau_{\tilde{\mathbf{X}}_i^\omega} \omega(i\Delta t)) P_0(d\chi) d\mathbf{y}, \\ &= \int_{R^d} p_0(\mathbf{0}, \mathbf{y}) \sigma \mathbf{y} \otimes E \boldsymbol{\psi} d\mathbf{y} = 0. \end{aligned} \quad (61)$$

where the last two equations in (61) come from Lemma 3.5 and $\tilde{\mathbf{X}}_i^\omega = \mathbf{X}_{i-1}^\omega + \mathbf{b}_{\Delta t}^{\omega((i-1)\Delta t)}(\mathbf{X}_{i-1}^\omega) + \sigma \tilde{\boldsymbol{\xi}}_{i-1}$ with another i.i.d $\tilde{\boldsymbol{\xi}}_{i-1}$ as before.

For the first term on the last line of (60), i.e., $\mathbf{E} \tilde{\mathbf{B}}_{\Delta t}^{\omega((i-1)\Delta t)}(\mathbf{X}_{i-1}^\omega) \otimes \boldsymbol{\psi}_{\Delta t}^{\omega(i\Delta t)}(\mathbf{X}_i^\omega)$, notice that

$$\begin{aligned} & \mathbf{E} \tilde{\mathbf{B}}_{\Delta t}^{\omega((i-1)\Delta t)}(\mathbf{X}_{i-1}^\omega) \otimes \boldsymbol{\psi}_{\Delta t}^{\omega(i\Delta t)}(\mathbf{X}_i^\omega) = \mathbf{E} \tilde{\mathbf{B}}_{\Delta t}(\eta_{n-1}) \otimes \mathbf{E}_{\eta_{n-1}} \boldsymbol{\psi}_{\Delta t}(\eta'_1), \\ &= \mathbf{E} \tilde{\mathbf{B}}_{\Delta t}(\eta_{n-1}) \otimes S_1 \boldsymbol{\psi}_{\Delta t}(\eta_{n-1}) = \mathbf{E} \tilde{\mathbf{B}}_{\Delta t}(\eta_{n-1}) \otimes (\boldsymbol{\psi}_{\Delta t}(\eta_{n-1}) - \tilde{\mathbf{B}}_{\Delta t}(\eta_{n-1})). \end{aligned} \quad (62)$$

From the property that S_i is measure-preserving 3.4, we have

$$\frac{1}{n} \sum_{i=1}^n \mathbf{E} \tilde{\mathbf{B}}_{\Delta t}^{\omega((i-1)\Delta t)}(\mathbf{X}_{i-1}^\omega) \otimes \boldsymbol{\psi}_{\Delta t}^{\omega(i\Delta t)}(\mathbf{X}_i^\omega) = \mathbf{E} \tilde{\mathbf{B}}_{\Delta t} \otimes \boldsymbol{\psi}_{\Delta t} - \mathbf{E} \tilde{\mathbf{B}}_{\Delta t} \otimes \tilde{\mathbf{B}}_{\Delta t}. \quad (63)$$

Thus, we get that

$$\lim_{n \rightarrow \infty} \frac{\mathbf{E}\bar{\mathbf{X}}_n^\omega \otimes \bar{\mathbf{X}}_n^\omega}{n\Delta t} = \sigma^2 \mathbf{I}_d + 2\mathbf{S}\mathbf{E}\boldsymbol{\psi}_{\Delta t} \otimes \tilde{\mathbf{b}}_{\Delta t}/\Delta t + O((\Delta t)). \quad (64)$$

Since the exponential-decay rate for S_n is $\exp(-c_1 n \Delta t)$, we know that the convergence rate for the above convergence is $\frac{1}{n} \frac{1 - \exp(-c_1 n \Delta t)}{1 - \exp(-c_1 \Delta t)} = O(\frac{1}{c_1 n \Delta t})$. Finally, according to Theorem 4.2, we have the estimate

$$\|2\mathbf{S}\mathbf{E}\boldsymbol{\psi}_{\Delta t} \otimes \tilde{\mathbf{B}}_{\Delta t}/\Delta t - 2\mathbf{S}\mathbf{E}\boldsymbol{\psi} \otimes \mathbf{b}\|_{L^2(\mathbf{x})} = \rho(\Delta t), \quad (65)$$

where $\lim_{\Delta t \rightarrow 0} \rho(\Delta t) = 0$. Thus, the statement in (54) is proved. \square

Notice that in the Theorem 4.3, we assume $\bar{\mathbf{X}}_n^\omega = \mathbf{X}_n^\omega - n\bar{\mathbf{B}}_{\Delta t}$ are given. In practice, we cannot calculate the drift term $\bar{\mathbf{B}}_{\Delta t}$ exactly. Therefore, we directly estimate the term $\mathbf{E}\mathbf{X}_n^\omega \otimes \mathbf{X}_n^\omega$, which is stated in the following corollary.

Corollary 4.4. *Let \mathbf{X}_n^ω , $n = 0, 1, \dots$ be the numerical solution obtained by using our numerical scheme and Δt denote the time-step. Suppose $n(\Delta t)^3$ is small enough, we have*

$$\frac{\mathbf{E}\mathbf{X}_n^\omega \otimes \mathbf{X}_n^\omega}{n\Delta t} = \sigma^2 I_n + 2\mathbf{S} \int_{\mathbf{X}} \boldsymbol{\psi} \otimes \mathbf{b} dP_0 + \rho(\Delta t) + O(\frac{1}{n\Delta t}) + O(n(\Delta t)^3), \quad (66)$$

where $\rho(\Delta t)$ is a function satisfying $\lim_{\Delta t \rightarrow 0} \rho(\Delta t) = 0$ and independent of the computational time T , and the \mathbf{S} represents the symmetrization operator.

Proof. Using the observation that

$$\frac{\mathbf{E}\mathbf{X}_n^\omega \otimes \mathbf{X}_n^\omega}{n\Delta t} = \frac{\mathbf{E}\bar{\mathbf{X}}_n^\omega \otimes \bar{\mathbf{X}}_n^\omega}{n\Delta t} + \frac{2\mathbf{S}\mathbf{E}\bar{\mathbf{X}}_n^\omega \otimes \bar{\mathbf{B}}_{\Delta t}}{\Delta t} + \frac{n^2 \bar{\mathbf{B}}_{\Delta t} \otimes \bar{\mathbf{B}}_{\Delta t}}{n\Delta t} \quad (67)$$

and the proposition 3.7, we can straightforwardly get the proof. \square

Remark 4.2. Corollary 4.4 shows that given a fixed time-step Δt ,

$$\lim_{n \rightarrow \infty} \frac{\mathbf{E}\mathbf{X}_n^\omega \otimes \mathbf{X}_n^\omega}{n\Delta t} = \sigma^2 \mathbf{I}_d + 2\mathbf{S} \int_{\mathbf{x}} \boldsymbol{\psi} \otimes \mathbf{b} dP_0 + \rho(\Delta t), \quad (68)$$

which reveals the connection of the definition of the effective diffusivity by solving discrete-type and continuous-type corrector problems.

Remark 4.3. In our convergence analysis, we interpret the solution process generated by our numerical scheme as a Markov process. By using the central limit theorem for the solution process (i.e., Markov process), we give a sharp error estimate of the proposed numerical scheme in computing effective diffusivity. If one chooses the Gronwall inequality in the error estimate, one cannot get rid of the exponentially growth prefactor in the error term.

5. Numerical Results

The aim of this section is two-fold. First, we will verify the convergence results obtained in Section 4.2. Second, we will use the proposed method to compute effective diffusivity in random flows. Incompressible random flows in two- and three-dimensional space will be studied. Without loss of generality, we compute the quantity $\frac{\mathbf{E}[(\mathbf{X}_{n,1}^\omega)^2]}{2n\Delta t}$, which is used to approximate D_{11}^E in the effective diffusivity matrix D^E . Notice that $\mathbf{X}_{n,1}^\omega$ is the first component of the vector \mathbf{X}_n^ω . One can obtain D_{11}^E by choosing $\mathbf{v} = (1, 0)^T$ in the equation (16) of the Prop. 2.5.

5.1. Numerical methods for generating random flows

To start with, we discuss how to generate random flows that will be used in our numerical experiments. Assume the vector field $\mathbf{b}(t, \mathbf{X}(t), \omega)$ has a spectral measure

$$\exp(-r(\mathbf{k})|t|)\Gamma(\mathbf{k})(\mathbf{I} - \frac{\mathbf{k} \otimes \mathbf{k}}{|\mathbf{k}|^2}), \quad (69)$$

where $\mathbf{k} = (k_1, k_2)^T$ or $\mathbf{k} = (k_1, k_2, k_3)^T$, $r(\mathbf{k}) > c_0$ for some positive constant c_0 , and $\Gamma(\mathbf{k})$ is integrable and decays fast for large \mathbf{k} . Under such settings, the velocity field $\mathbf{b}(t, \mathbf{X}(t), \omega)$ satisfies the ρ mixing condition and is stationary and divergence free [16, 4]. In order to mimic the energy spectrum of real flows, we assume $\Gamma(\mathbf{k}) \propto 1/|\mathbf{k}|^{2\alpha+d-2}$ with ultraviolet cutoff $|\mathbf{k}| \leq K < \infty$ and $r(\mathbf{k}) \propto |\mathbf{k}|^{2\beta}$. The spectral gap condition 4 requires $\beta \leq 0$ and the integrability of $\Gamma(\mathbf{k})$ requires $\alpha < 1$. Here for simplicity, we choose $\beta = 0$.

Given the spectral measure (69), we use the randomization method [11, 13] to generate realizations of the velocity field. Specifically, we approximate it as

$$\mathbf{b}(t, \mathbf{x}) = \frac{1}{\sqrt{M}} \sum_{m=1}^M [\mathbf{u}_m \cos(\mathbf{k}_m \cdot \mathbf{x}) + \mathbf{v}_m \sin(\mathbf{k}_m \cdot \mathbf{x})]. \quad (70)$$

Notice that we have suppressed the dependence of the velocity on ω for notation simplicity here. In fact, the parameters \mathbf{k}_m , \mathbf{u}_m and \mathbf{v}_m contain randomness. The spectrum points \mathbf{k}_m were chosen independently according to the spectral measure $\Gamma(\mathbf{k})$. Due to the isotropicity, we first generate a point uniformly distributed on the unit sphere or unit circle, which represents the direction of the \mathbf{k}_m . Then we generate the length r of \mathbf{k}_m , which satisfies a density function $\rho(r) \propto 1/r^{2\alpha-1}$, $0 < r \leq K$.

For the random flows in two-dimensional space, we have

$$\mathbf{u}_m = \xi_m(t) \frac{\mathbf{k}_m^\perp}{|\mathbf{k}_m^\perp|}, \quad \mathbf{v}_m = \eta_m(t) \frac{\mathbf{k}_m^\perp}{|\mathbf{k}_m^\perp|}, \quad \mathbf{k}_m = (k_m^1, k_m^2), \quad m = 1, \dots, M, \quad (71)$$

where $\mathbf{k}_m^\perp = (-k_m^2, k_m^1)$, $\xi_m(t)$ and $\eta_m(t)$ are independent 1D Ornstein-Uhlenbeck (OU) processes with covariance function $Cov(\xi_m(t_1), \xi_m(t_2)) = Cov(\eta_m(t_1), \eta_m(t_2)) = \exp(-\theta|t_1 - t_2|)$. Here $\theta > 0$ is a parameter to control the roughness of the OU process. To obtain the OU path for $\xi_m(t)$, we generate a series of $\{\xi_m(n\Delta t)\}$ satisfies

$$\xi_m(n\Delta t) = e^{-\theta\Delta t} \xi_m((n-1)\Delta t) + \sqrt{1 - e^{-2\theta\Delta t}} \zeta_n, \quad n = 1, 2, 3, \dots \quad (72)$$

where $\xi_m(0)$, ζ_n $n = 1, 2, 3, \dots$ are i.i.d. $N(0, 1)$ distributed random variables. One can easily verify that $Cov(\xi_m(i\Delta t), \xi_m(j\Delta t)) = \exp(-\theta|i - j|\Delta t)$. The OU path for $\eta_m(t)$ can be generated by using the same approach.

For the random flows in three-dimensional space, we have

$$\mathbf{u}_m = \boldsymbol{\xi}_m(t) \times \frac{\mathbf{k}_m}{|\mathbf{k}_m|}, \quad \mathbf{v}_m = \boldsymbol{\eta}_m(t) \times \frac{\mathbf{k}_m}{|\mathbf{k}_m|}, \quad \mathbf{k}_m = (k_m^1, k_m^2, k_m^3), \quad (73)$$

where the samples $\boldsymbol{\xi}_m(t)$ and $\boldsymbol{\eta}_m(t)$ are independent 3D random vectors, whose components are independent stationary OU process having the covariance function $Cov(\boldsymbol{\xi}_m(t_1), \boldsymbol{\xi}_m(t_2)) = Cov(\boldsymbol{\eta}_m(t_1), \boldsymbol{\eta}_m(t_2)) = \exp(-\theta|t_1 - t_2|)\mathbf{I}_3$. Each component of $\boldsymbol{\xi}_m(t)$ and $\boldsymbol{\eta}_m(t)$ can be generated by using the method (72). One can easily verify that in both the 2D and 3D cases the velocity fields generated by (70) satisfy the divergence free condition.

5.2. Verification of the convergence analysis

In this subsection, we study the convergence rate of our method in computing incompressible random flow in 2D and 3D space.

For the random flow in 2D space, we solve the SDE (1), where the velocity field is chosen as (70) with the setting (71). The velocity field were simulated with $M = 1000$. The parameters in the spectral measure $\Gamma(\mathbf{k})$ are $K = 10$ and $\alpha = 0.75$. The time-mixing constant $\theta = 10$ in the covariance function. The molecular diffusivity $\sigma = 0.1$. We use Monte Carlo method to generate dependent samples for the Brownian motion $\mathbf{w}(t)$ and velocity field $\mathbf{b}(t, \mathbf{x})$. The sample number is denoted by N_{mc} . We choose $\Delta t_{ref} = 0.001$ and $N_{mc} = 100,000$ to solve the SDE (1) and compute the reference solution, i.e., the ‘‘exact’’ effective diffusivity, where the final computational time is $T = 22$ so that the calculated effective diffusivity converges to a constant. It takes about 24 hours to compute the reference solution on a 64-core server (Gridpoint System at HKU). The reference solution for the effective diffusivity is $D_{11}^E = 0.1736$.

For the random flow in 3D space, we solve the SDE (1), where the velocity field is chosen as (70) with the setting (73). The velocity field were simulated with $M = 100$. The parameters in the spectral measure $\Gamma(\mathbf{k})$ are $K = 10$ and $\alpha = 0.75$. The time-mixing constant $\theta = 10$ in the covariance function. The molecular diffusivity $\sigma = 0.1$. Again, we use Monte Carlo method to generate dependent samples for the Brownian motion $\mathbf{w}(t)$ and velocity field $\mathbf{b}(t, \mathbf{x})$. We choose $\Delta t_{ref} = 0.001$ and $N_{mc} = 180,000$ to solve the SDE (1) and compute the reference solution, i.e., the ‘‘exact’’ effective diffusivity, where the final computational time is $T = 25$ so that the calculated effective diffusivity converges to a constant. It takes about 21 hours to compute the reference solution on a 64-core server (Gridpoint System at HKU). The reference solution for the effective diffusivity is $D_{11}^E = 0.1137$. We remark that in our numerical experiment, we choose $M = 1000$ for 2D random flow and $M = 100$ for 3D random flow so that the velocity field numerically satisfies the ergodicity assumption.

In Fig.1a, we plot the convergence results of the effective diffusivity for the 2D random flow using our method (i.e., $\frac{E[(\mathbf{X}_{n,1}^\omega)^2]}{2n\Delta t}$) with respect to different time-step Δt at $T = 22$, where the number of the Monte Carlo samples $N_{mc} = 50,000$. In addition, we show a fitted

straight line with the slope 1.17, i.e., the convergence rate is about $O(\Delta t)^{1.17}$. Similarly, we show the convergence results of $\frac{E[(\mathbf{X}_{n,1}^\omega)^2]}{2n\Delta t}$ for the 3D random flow in Fig.1b with respect to different time-step Δt at $T = 25$, where the number of the Monte Carlo samples $N_{mc} = 50,000$. We also show a fitted straight line with the slope 0.98, i.e., the convergence rate is about $O(\Delta t)^{0.98}$. These numerical results agree with our error analysis.

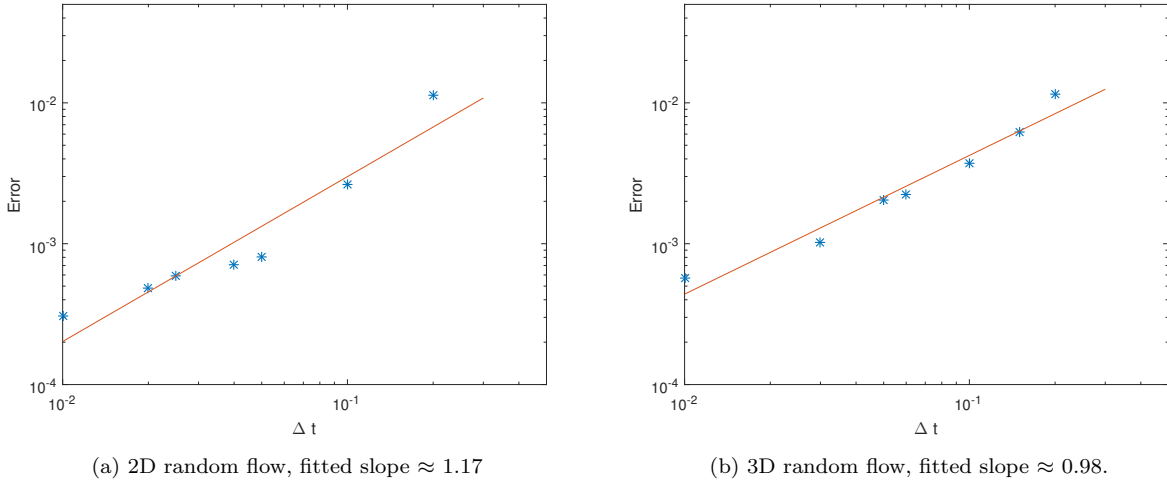


Figure 1: Error of D_{11}^E for random flows with different time-steps.

5.3. Verification of the exponential decay property.

The time relaxation property (4), which is equivalent to the exponential decay property (5), plays an important role in the existence of the effective diffusivity; see Prop. 2.5. In Theorem 3.6, we prove that the numerical solution inherits the exponential decay property. Based on this key fact, we can define the discrete-type corrector problem and prove the convergence analysis of our method. In this subsection, we will verify that the velocity field propagated by the random flow (70) has the exponential decay property, where both the 2D and 3D cases will be tested.

In the experiment for 3D random flow, we choose the time step size $\Delta t = 0.05$. The velocity field will be approximated by $M = 100$ terms in (70). The parameters in the spectral measure $\Gamma(\mathbf{k})$ are $K = 10$ and $\alpha = 0.75$. The molecular diffusivity $\sigma = 0.1$. We randomly generate 200 samples $\{\mathbf{k}_m^i, \boldsymbol{\xi}_m^i(0), \boldsymbol{\eta}_m^i(0), m = 1, \dots, M\}$, $i = 1, \dots, 200$, which will be used to generate initial states for the velocity field (70), i.e.,

$$\mathbf{b}^i(0, \mathbf{x}) = \frac{1}{\sqrt{M}} \sum_{m=1}^M \left[\boldsymbol{\xi}_m^i(0) \times \frac{\mathbf{k}_m^i}{|\mathbf{k}_m^i|} \cos(\mathbf{k}_m^i \cdot \mathbf{x}) + \boldsymbol{\eta}_m^i(0) \times \frac{\mathbf{k}_m^i}{|\mathbf{k}_m^i|} \sin(\mathbf{k}_m^i \cdot \mathbf{x}) \right], \quad i = 1, \dots, 200.$$

Then for each initial state $\mathbf{b}^i(0, \mathbf{x})$, we generate 5000 different samples of the OU paths $\boldsymbol{\xi}_m^{i,p}(n\Delta t)$ and $\boldsymbol{\eta}_m^{i,p}(n\Delta t)$ and Brownian motion paths $\mathbf{w}^{i,p}(n\Delta t)$, $1 \leq p \leq 5000$. Given the

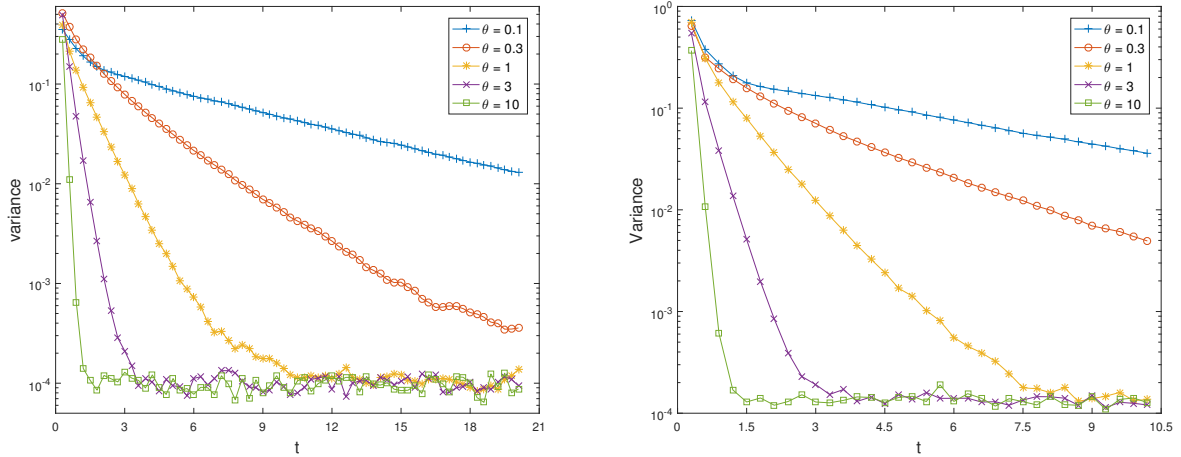
sample data, we calculate the corresponding solution paths $\{\mathbf{X}_n^{i,p}\}_{0 \leq n < \infty}$ and then calculate the value

$$\mathbf{b}^{i,p}(n\Delta t, \mathbf{X}_n^{i,p}) = \frac{1}{\sqrt{M}} \sum_{m=1}^M [\boldsymbol{\xi}_m^{i,p}(n\Delta t) \times \frac{\mathbf{k}_m^i}{|\mathbf{k}_m^i|} \cos(\mathbf{k}_m^i \cdot \mathbf{X}_n^{i,p}) + \boldsymbol{\eta}_m^i(n\Delta t) \times \frac{\mathbf{k}_m^i}{|\mathbf{k}_m^i|} \sin(\mathbf{k}_m^i \cdot \mathbf{X}_n^{i,p})],$$

$$i = 1, \dots, 200, \quad 1 \leq p \leq 5000. \quad (74)$$

Finally, we compute $\bar{\mathbf{b}}_n^i = \frac{1}{5000} \sum_{p=1}^{5000} \mathbf{b}^{i,p}(n\Delta t, \mathbf{X}_n^{i,p})$ and calculate the variance of $\bar{\mathbf{b}}_n^i$ with respect to i . The experiment for 2D random flow is almost the same except the setting of the velocity field (70) is replaced by (71) and we choose $M = 1000$.

In Fig. 2a and Fig. 2b, we plot the calculated sample variance of the first component of $\bar{\mathbf{b}}_n^i$ for the 2D random flow and 3D random flow, respectively. We observe exponential decay of the sample variance with respect to time. Moreover, we find that larger θ leads to a faster decay in the sample variance, since larger θ results in a fast decorrelation in the random flow. Our numerical results show that the exponential decay property (see Theorem 3.6) holds for the random flows we studied here.



(a) Calculated variance in the 2D flow along time.

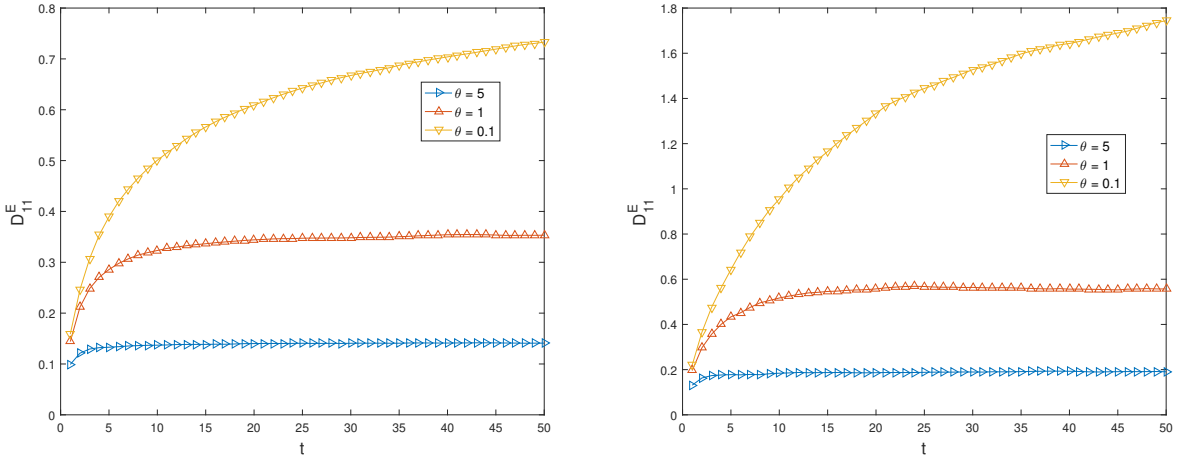
(b) Calculated variance in the 3D flow along time.

Figure 2: Decay behaviors of the sample variance in 2D and 3D random flows.

5.4. Investigation of the convection-enhanced diffusion phenomenon

We first study the relation between the numerical effective diffusivity $\frac{E[(\mathbf{X}_{n,1}^\omega)^2]}{2n\Delta t}$ and the parameter θ , which controls the de-correlation rate in the time space of the random flow. In this experiment, the setting of the velocity field and the implementation of our method is the same as we used in Section 5.3. We only choose different parameter θ to compute the numerical effective diffusivity.

In Fig. 3a, we plot the numerical effective diffusivity of 2D random flow obtained at different computational times, where the flow is generated with different θ . The result for



(a) The quantity $\frac{E[(\mathbf{X}_{n,1}^\omega)^2]}{2n\Delta t}$ in the 2D flow along time.

(b) The quantity $\frac{E[(\mathbf{X}_{n,1}^\omega)^2]}{2n\Delta t}$ in the 3D flow along time.

Figure 3: The relation between numerical effective diffusivity and θ .

3D random flow is shown in Fig. 3b. We find that different θ affects the mixing time of the system. When we increase the θ , the system will quickly enter a mixing stage.

Finally, we choose different molecular diffusivity σ to compute the corresponding numerical effective diffusivity, which allows us to study the existence of residual diffusivity for this random flow. The residual diffusivity, a special yet remarkable convection-enhanced diffusion phenomenon, refers to the non-zero and finite effective diffusivity in the limit of zero molecular diffusivity as a result of a fully chaotic mixing of the streamlines.

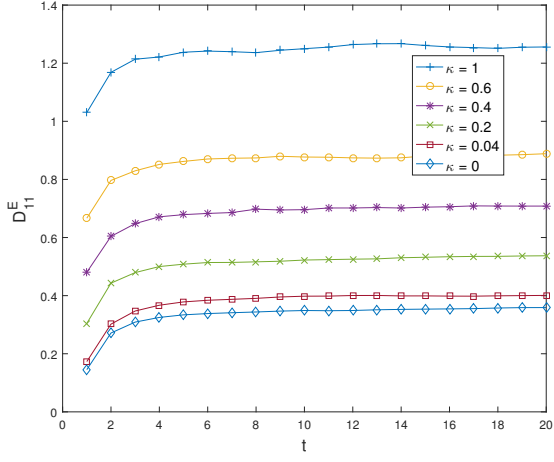
In the experiment for 2D random flow, we choose the time step size $\Delta t = 0.05$, the velocity field were simulated with $M = 1000$, the time-mixing constant $\theta = 0.1$ and the parameters in the spectral measure $\Gamma(\mathbf{k})$ are $K = 10$ and $\alpha = 0.75$. For the 3D random flow, we choose $M = 100$ and keep other parameters the same.

Let $\kappa = \sigma^2/2$. In Fig.4a, we show the relation between numerical effective diffusivity of 2D random flow obtained at different computational times, where the result is generated with different σ . The result for 3D random flow is shown in Fig. 4b. We find that as κ approaches zero, the quantity $\frac{E[(\mathbf{X}_{n,1}^\omega)^2]}{2n\Delta t}$ converges to a non-zero (positive) constant, which indicates the existence of residual diffusivity in the random flows here.

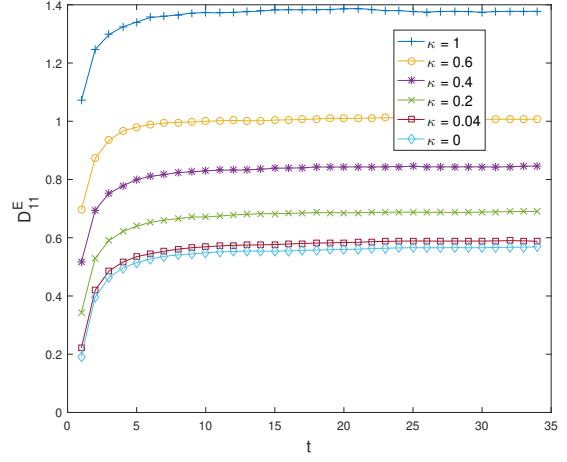
In Fig.5a and Fig.5b, we plot the convergence behaviors of $D_{11}^E(\kappa)$ approaching $D_{11}^E(0)$ for the 2D and 3D random flows, respectively, when the systems enter a mixing stage. The convergence behaviors when κ approaches zero are slightly different though, both figures show that residual diffusivity exists in the random flows we studied here.

6. Conclusion

In this paper, we studied the numerical homogenization of passive tracer models in random flows. Based on a splitting method, we proposed stochastic structure-preserving schemes to compute the effective diffusivity of the random flows. In addition, we provided rigorous

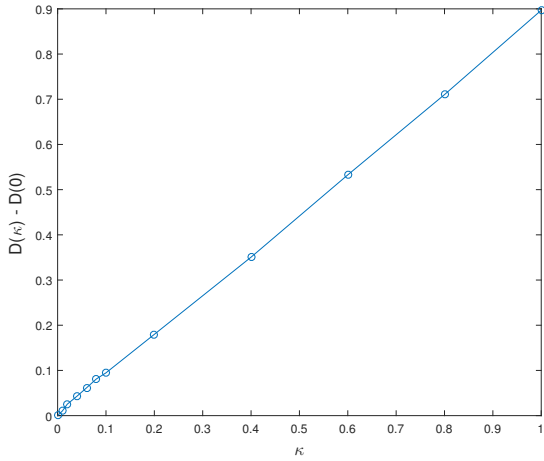


(a) The quantity $\frac{E[(\mathbf{X}_{n,1}^\omega)^2]}{2n\Delta t}$ in the 2D flow along time.

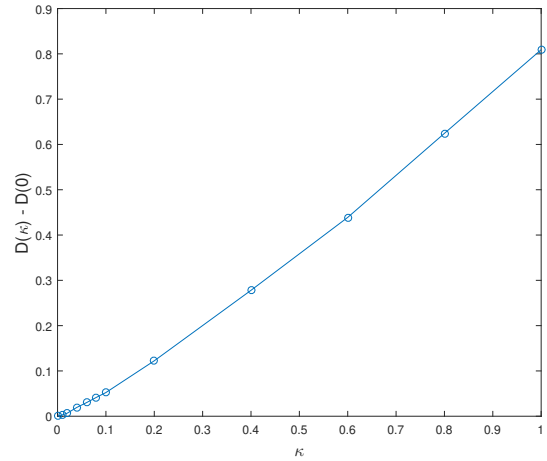


(b) The quantity $\frac{E[(\mathbf{X}_{n,1}^\omega)^2]}{2n\Delta t}$ in the 3D flow along time.

Figure 4: The relation between numerical effective diffusivity and molecular diffusivity σ .



(a) Results for the 2D random flow.



(b) Results for the 3D random flow.

Figure 5: Convergence behaviors of $D_{11}^E(\kappa)$ approaching $D_{11}^E(0)$.

convergence analysis for the numerical schemes. Our error analysis is completely new in the sense that it is based on a probabilistic approach. Specifically, we interpreted the solution process generated by our numerical schemes as a Markov process. By using the central limit theorem for the solution process, we gave a sharp error estimate for our numerical schemes in computing the effective diffusivity. Finally, we present numerical results to verify the convergence rate of the proposed method for incompressible random flows both in 2D and 3D spaces. In addition, we observed the exponential decay property and investigated the residual diffusivity phenomenon in the random flows we studied here.

There are two directions we plan to explore in our future work. First, we shall extend the probabilistic approach to provide sharp convergence analysis in computing effective diffusivity for time-dependent chaotic flows, such as time-dependent ABC flows. In addition, we shall investigate the convection-enhanced diffusion phenomenon for general spatial-temporal stochastic flows [12, 13] and develop convergence analysis for the corresponding numerical methods.

Acknowledgement

The research of J. Lyu and Z. Wang are partially supported by the Hong Kong PhD Fellowship Scheme. The research of J. Xin is partially supported by NSF grants DMS-1211179, DMS-1522383, and IIS-1632935. The research of Z. Zhang is supported by Hong Kong RGC grants (Projects 27300616, 17300817, and 17300318), National Natural Science Foundation of China (Project 11601457), Seed Funding Programme for Basic Research (HKU), and Basic Research Programme (JCYJ20180307151603959) of The Science, Technology and Innovation Commission of Shenzhen Municipality. The computations were performed using the HKU ITS research computing facilities that are supported in part by the Hong Kong UGC Special Equipment Grant (SEG HKU09).

References

- [1] A. BENSOUSSAN, J. L. LIONS, AND G. PAPANICOLAOU, *Asymptotic analysis for periodic structures*, vol. 374, American Mathematical Soc., 2011.
- [2] R. CARMONA AND L. XU, *Homogenization for time-dependent two-dimensional incompressible Gaussian flows*, *The Annals of Applied Probability*, 7 (1997), pp. 265–279.
- [3] P. DEDIK AND M. SUBIN, *Random pseudodifferential operators and the stabilization of solutions of parabolic equations with random coefficients.*, *Sbornik: Mathematics*, 41 (1982), pp. 33–52.
- [4] P. DOUKHAN, *Mixing: properties and examples*, vol. 85, Springer Science & Business Media, 2012.

- [5] A. FANNJIANG AND T. KOMOROWSKI, *Turbulent diffusion in markovian flows*, The Annals of Applied Probability, 9 (1999), pp. 591–610.
- [6] A. FANNJIANG AND G. PAPANICOLAOU, *Diffusion in turbulence*, Probability Theory and Related Fields, 105 (1996), pp. 279–334.
- [7] J. GARNIER, *Homogenization in a periodic and time-dependent potential*, SIAM Journal on Applied Mathematics, 57(1) (1997), pp. 95–111.
- [8] V. V. JIKOV, S. KOZLOV, AND O. A. OLEINIK, *Homogenization of Differential Operators and Integral Functionals*, Springer, Berlin, 1994.
- [9] P. E. KLOEDEN AND E. PLATEN, *Numerical solution of Stochastic Differential Equations*, Springer-Verlag Berlin, Heidelberg, 1992.
- [10] T. KOMOROWSKI AND S. OLLA, *On homogenization of time-dependent random flows*, Probability theory and related fields, 121 (2001), pp. 98–116.
- [11] R. KRAICHNAN, *Diffusion by a random velocity field*, The physics of fluids, 13 (1970), pp. 22–31.
- [12] C. LANDIM, S. OLLA, AND H. YAU, *Convection–diffusion equation with space–time ergodic random flow*, Probability theory and related fields, 112 (1998), pp. 203–220.
- [13] A. J. MAJDA AND P. R. KRAMER, *Simplified models for turbulent diffusion: theory, numerical modelling, and physical phenomena*, Phys. Rep., 314 (1999), pp. 237–574.
- [14] G. PAVLIOTIS AND A. STUART, *Multiscale methods: averaging and homogenization*, Springer Science and Business Media, 2008.
- [15] G. PAVLIOTIS, A. STUART, AND K. ZYGALAKIS, *Calculating effective diffusivities in the limit of vanishing molecular diffusion*, J. Comput. Phys., 228 (2009), pp. 1030–1055.
- [16] M. ROSENBLATT, *Markov Processes: Structure and Asymptotic Behavior*, vol. 184, Springer Science & Business Media, 2012.
- [17] G. STRANG, *On the construction and comparison of difference schemes*, SIAM J. Numer. Anal., 5 (1968), pp. 506–517.
- [18] Z. WANG, J. XIN, AND Z. ZHANG, *Sharp uniform in time error estimate on a stochastic structure-preserving Lagrangian method and computation of effective diffusivity in 3D chaotic flows*, arXiv:1808.06309, (2018).
- [19] Z. J. WANG, J. XIN, AND Z. W. ZHANG, *Computing effective diffusivity of chaotic and stochastic flows using structure-preserving schemes*, SIAM Journal on Numerical Analysis, 56 (2018), pp. 2322–2344.